Master's thesis

NTNU
Norwegian University of Science and Technology
Faculty of Natural Sciences
Department of Physics

Ingrid Mardal

Impact of overall charge and charge distribution in disordered regions on the binding between DNA and DNA-binding molecules containing disordered regions

Master's thesis in Applied Physics and Mathematics
Supervisor: Rita de Sousa Dias
February 2021

NTNU
Norwegian University of
Science and Technology

Ingrid Mardal

Impact of overall charge and charge distribution in disordered regions on the binding between DNA and DNA-binding molecules containing disordered regions

Master's thesis in Applied Physics and Mathematics
Supervisor: Rita de Sousa Dias
February 2021

Norwegian University of Science and Technology
Faculty of Natural Sciences
Department of Physics

Abstract

The interactions between DNA-binding proteins and DNA are highly important in many cellular processes. Until recently, it has been believed that the function of proteins is directly dependent on their well-defined, three-dimensional structure. Intrinsically disordered regions (IDRs) lack these requirements, but there is growing evidence for their importance in proteins, especially DNA-binding proteins. Within this context, IDRs include both disordered tails and flexible linkers, which are disordered regions connected to one or two DNA-binding domains (DBDs), respectively. They can affect both the specificity and affinity of the protein to DNA, and thereby play a crucial role in the interactions between them. However, the underlying molecular mechanisms of IDRs are not fully understood.

In this work, the effect of overall charge and charge distribution in disordered regions on the binding between DNA and DNA-binding molecules was investigated. The DBDs were mimicked using positively charged PAMAM dendrimers, which bind non-specifically to the negatively charged DNA. Peptides of various charge and charge distributions were conjugated to the dendrimers, mimicking IDRs. The resulting structures were assessed by mass spectrometry, but the exact molecule structures were not possible to determine. However, the results strongly suggest that the peptides conjugated to the dendrimers. The interactions between the resulting conjugates and DNA were studied using dye exclusion assays and gel electrophoresis. For the conjugates possessing negatively charged peptides, DNA condensation was not observed. This suggests that the peptides invert the charge of the PAMAM, preventing it from binding to DNA by electrostatic repulsion. Conjugates with neutral or approximately neutral peptides showed a much weaker DNA condensation compared to non-conjugated PAMAM. The results indicate that the conjugates bind to DNA, but the tails hinder condensation to some degree. For the conjugates possessing positively charged peptides, condensation of DNA was either increased or remained constant, compared to condensation by the non-conjugated dendrimers. In addition, peptides with different amino acid distributions, with the same total positive charge, were investigated. Unfortunately, it was not possible to draw significant conclusions regarding the effect of amino acid architecture on the binding between DNA and conjugates.

Sammendrag

Samspillet mellom DNA-bindende proteiner og DNA er svært viktig i mange cellulære prosesser. Inntil nylig har det vært antatt at proteiners funksjon er direkte avhengig av deres veldefinerte, tredimensjonale struktur. Iboende ustrukturerte regioner mangler disse spesifikasjonene, men det fremkommer stadig flere beviser på deres nødvendige roller i proteiner, da spesielt DNA-bindende proteiner. I denne sammenhengen kan disse regionene bestå av både ustrukturerte haler og fleksible lenker, som er ustrukturerte regioner koblet til henholdsvis ett eller to DNA-bindende domener. De kan påvirke både spesifisiteten og affiniteten til proteinet for DNA, og dermed spille en avgjørende rolle i samspillet mellom dem. Imidlertid er de underliggende molekylære mekanismene til de ustrukturerte regionene ikke fullt ut forstått. I dette arbeidet ble effekten av totalladning og ladningsfordeling i ustrukturerte regioner på bindingen mellom DNA and DNA-bindende molekyler undersøkt. De DNA-bindende domenene ble etterlignet ved bruk av positivt ladede PAMAM dendrimerer, som binder uspesifikt til negativt ladet DNA. Peptider med forskjellige ladninger og ladningsfordelinger imiterte de ustrukturerte regionene og ble konjugert til dendrimerene. De resulterende strukturene ble analysert ved bruk av massespektrometri, men den nøyaktige molekylstrukturen var ikke mulig å bestemme. Eksperimentene antydet likevel at dendrimerene og peptidene hadde konjugert. Interaksjonene mellom de resulterende konjugatene og DNA ble studert ved bruk av fargestoffekskluderingsanalyser og gelelektroforese. DNA-kondensasjon ble ikke observert for konjugatene med negativt ladede peptider. Dette antyder at peptidene inverterer ladningen til PAMAM, og forhindrer at den blir bundet til DNA ved elektrostatisk frastøting. Konjugater med nøytrale eller tilnærmet nøytrale peptider viste en mye svakere DNA-kondensasjon sammenlignet med ikke-konjugert PAMAM. Resultatene indikerer at konjugatene binder seg til DNA, men de ustrukturerte halene hindrer kondensasjonen til en viss grad. For konjugatene med positivt ladede peptider ble kondensering av DNA enten økt eller holdt konstant, sammenlignet med kondenseringen av ikke-konjugerte dendrimerer. I tillegg ble peptider med forskjellige aminosyredistribusjoner, med samme totale positive ladning, undersøkt. Dessverre var det ikke mulig å trekke signifikante konklusjoner angående effekten av aminosyrearkitektur på bindingen mellom DNA og konjugater.

Preface

This Master's thesis was written at the end of my studies at the program Applied Physics and Mathematics at the Norwegian University of Science and Technology.

I would like to thank my supervisor, Rita de Sousa Dias, for her extraordinary guidance and support during this thesis and project work in spring 2020. I would also like to thank PhD student Corinna Dannert for valuable discussions and guidance in the laboratory work. Thanks also to Gjertrud Maurstad, for providing materials for my laboratory work, and to Kåre Andre Kristiansen for performing the mass spectrometry experiments. Lastly, I want to thank my family, boyfriend and friends for their continuous support during the entire process.

Unfortunately, the pandemic affected the thesis work due to the lack of laboratory practice in the project work during spring 2020. All laboratory work, experiments and optimizations of procedures were therefore performed in this thesis during fall 2020.

Table of Contents

Abstract **i**

Sammendrag **ii**

Preface **iii**

Table of Contents **vii**

1 Introduction **1**

2 Theory **3**

2.1 Protein structure 3

2.1.1 Features of IDRs 5

2.2 DNA 6

2.2.1 DNA-protein interactions 6

2.2.2 Disordered regions in DNA-protein interactions 9

2.3 PAMAM dendrimers 10

2.3.1 DNA condensation by PAMAM dendrimers 11

3 Methods **13**

3.1 Fluorescence spectroscopy 13

3.2 UV/Vis spectroscopy 15

3.3 Gel electrophoresis 16

3.4 Mass spectrometry 17

4 Experimental procedures **19**

4.1 Materials and sample preparations 19
4.1.1 DNA 19
4.1.2 PAMAM dendrimers 19
4.1.3 Peptide sequences 20
4.1.4 Other materials 21
4.2 Conjugation of PAMAM dendrimers and peptides 22
4.2.1 PAMAM-SPDP-peptide conjugation 24
4.3 Characterization of PAMAM-peptide conjugates 27
4.3.1 Mass spectrometry 27
4.3.2 Agarose Gel electrophoresis and PageBlue Protein Staining 27
4.4 Fluorescence spectroscopy 28
4.4.1 Optimization of dye exclusion assay 28
4.4.2 Relationship between DNA concentration and fluorescence intensity 30
4.5 Gel electrophoresis 30

5 Results and Discussion 33

5.1 Conjugation of PAMAM dendrimers and peptides 33
5.1.1 Conjugation of PAMAM dendrimers and SPDP crosslinker 33
5.1.2 Conjugation of PAMAM-SPDP complexes and peptides 35
5.2 Characterization of PAMAM-peptide conjugates 39
5.2.1 Mass spectrometry 39
5.2.2 Gel electrophoresis with PageBlue Protein Staining Dye 46
5.2.3 Summary of characterization methods and future work 47
5.3 Dye exclusion assays 49
5.3.1 Relationship between DNA concentration and fluorescence intensity 49
5.3.2 Optimization of dye exclusion assay 50
5.3.3 Dye exclusion with PAMAM-peptide conjugates 51
5.4 Gel electrophoresis 58
5.4.1 Optimizing the sample concentration range 58
5.4.2 DNA condensation by peptides and PAMAM-peptide conjugates . . 60
5.5 Summary of gel electrophoresis and dye exclusion assays 65

6 Conclusion **69**

Bibliography **71**

Appendix **79**

A.1 Mass spectrometry - Full retention time 79

A.2 Additional dye exclusion assay of PAMAM-SN8-24 and DNA 80

Chapter 1

Introduction

Traditionally, the well-defined three-dimensional structure of proteins has been viewed as necessary in the performance of their biological function. However, several studies have in the last two decades revealed that large numbers of these proteins contain and depend on unstructured regions. These intrinsically disordered proteins (IDPs) and regions (IDRs) are involved in numerous cell activities, including cell signaling and regulation. In particular, IDRs are abundant in DNA-binding proteins and have been shown to play an important role in protein-DNA interactions [1, 2]. These interactions are crucial in several cellular processes, such as DNA transcription, DNA replication, and DNA recombination and repair [3].

Disordered tails and flexible linkers are types of IDRs, known for their impact on both specificity and affinity in protein-DNA interactions. Disordered tails, found at one or both ends of DNA-binding proteins, often undergo a disorder-to-order transition when binding to DNA. This increases the specificity of the DNA binding. In addition, the tails may support nonspecific protein-DNA interactions occurring when a protein is searching for DNA. Disordered flexible linkers are, on the other hand, often found between DNA-binding domains (DBDs). The linkers allow for the relative movement of the domains, while also mediating cooperation between them in DNA target search [4]. After the binding of one DBD to DNA, the flexible linker facilitates the binding of a second DBD by adjusting the orientation and separation of the domains. Consequently, it has been believed that the main function of the flexible linker is to indirectly regulate the interactions between the DNA-binding proteins and DNA. However, several recent studies suggest that the linker

interacts directly with DNA and plays a more "active" role in the control of protein-DNA interactions than first assumed [5].

Several IDPs are associated with diseases, such as cancer, and cardiovascular and neurodegenerative diseases [6]. For example, the multifunctional transcription factor p53 is a known IDP, possessing both a flexible linker and disordered tails [4]. p53 is a crucial regulator in several cellular processes, and around 50 % of human cancer cells have mutations in the p53 gene [7].

However, the molecular mechanisms of IDPs and IDRs and their structure-function relationship are still not fully understood. Knowledge regarding these issues will lead to a deeper understanding of their role in different cellular processes and diseases. Recent studies suggest that the presence or absence of charges in disordered regions, including both disordered tails and flexible linkers, notably affect the binding between proteins and DNA [4, 5].

The aim of this project was therefore to explore the impact of overall charge and charge distribution in disordered regions on the binding between DNA and DNA-binding molecules containing disordered regions. For simplicity, the DBDs in these molecules were mimicked using positively charged poly(amidoamine) (PAMAM) dendrimers, which bind non-specifically to DNA. Peptide sequences of various charge and amino acid composition were conjugated to the dendrimers, resembling disordered regions as either flexible linkers or tails. The extent of the conjugation was investigated using UV spectroscopy, and mass spectrometry was performed to assess the resulting molecules. The interactions between DNA and the conjugated dendrimers were assessed using dye exclusion assays and gel electrophoresis.

Chapter 2

Theory

2.1 Protein structure

Proteins are macromolecules essential in all organisms, which can be found almost everywhere in the cell. They are linear polymers composed of amino acids, with the amino acid sequence making up the polypeptide chain. Monomeric proteins consist of a single polypeptide, while multimeric proteins are made up of two or more polypeptides [3].

The amino acid sequence is referred to as the primary structure of the protein. The secondary structure arises from the folding into alpha helices or beta sheets, while the tertiary structure is formed when the polypeptide chain folds into a three-dimensional structure. The most stable three-dimensional conformation of a polypeptide chain is known as its native conformation. If proteins are multimeric, their chains may be brought together, resulting in a quaternary protein structure. Globular proteins, in contrast to fibrous proteins, fold into compact structures rather than extended filaments. The globular proteins are the most common type in the cellular structure. Many of them contain several units with defined local tertiary structures called domains. These domains often have a specific protein function, and large proteins usually consist of several domains [3].

The structure-function paradigm, formulated more than 100 years ago, states that the three-dimensional structure of a protein determines its specific biological function. However, this paradigm was re-assessed in the mid 1990s, when many biologically functioning proteins, without ordered, three-dimensional structures, were recognized. The unstructured segments of a protein are now referred to as IDRs, while the proteins containing

them are called IDPs [8, 9].

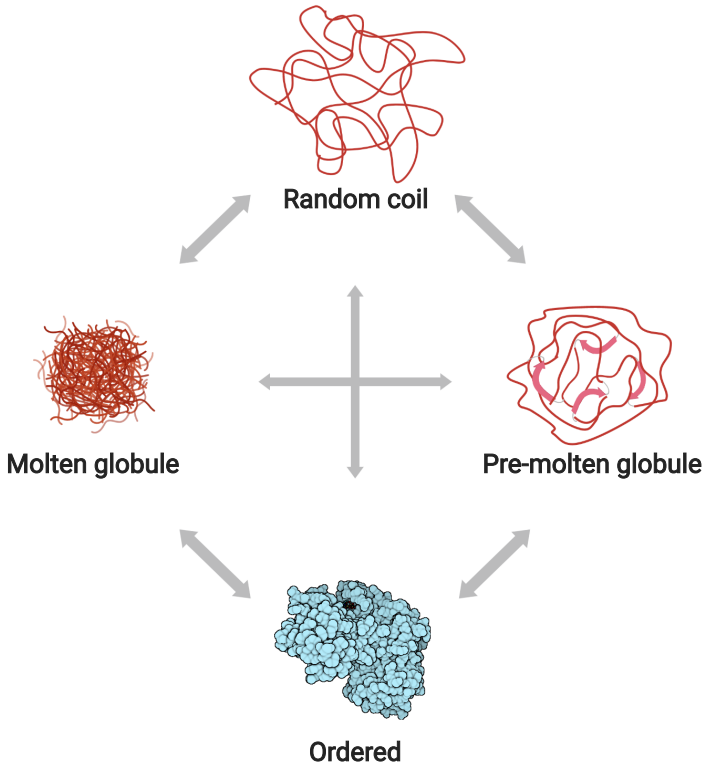

Figure 2.1: Protein quartet model. The model states that protein function depends on four different conformational states of the polypeptide chain and the transistions between them. The four states include the random coil, the pre-molten globule, the molten globule, and the ordered structure. Created with BioRender.com.

Protein structure may be described as a conformational continuum, ranging from entirely disordered to tightly folded structures. In the protein quartet model, the spectrum is divided into four different types, namely random coils, pre-molten globules, molten globules, and ordered structures [8], see Figure 2.1. According to this model, the protein function depends on these states and the transitions between them. The IDRs may fall into all categories, except for "Ordered". The random coil shows little or no secondary structure, while the pre-molten globule represents a more compact form of a coil, with local regions of the sequence adopting secondary structure. The molten globule has a native-like secondary structure and is even more compact than the pre-molten globule. However, its tertiary structure is still disordered. The protein structures defined as ordered have a well-defined three-dimensional structure [8, 10, 11].

2.1.1 Features of IDRs

The amino acid sequences of IDPs/IDRs differ in many ways from structured proteins and regions, including their charge, amino acid composition, hydrophobicity, flexibility, and aromaticity [6]. IDRs often show a low sequence complexity, meaning that the sequences frequently are composed of segments of the same amino acid or a mixture of a limited number of different types. Some may also consist of short-period regular repeats [9, 12]. The IDRs may be distinguished from more structured protein regions based on their amino acid composition. Amino acids such as cysteine(C), tryptophan(W), tyrosine(Y), isoleucine(I), and valine(V) are often seen in structured regions and referred to as order-promoting residues. Examples of disorder-promoting amino acids, frequently seen in IDRs, are arginine(R), lysine(K), glutamic acid(E), proline(P), and serine(S) [13, 14].

The hydrophobic effect is one of the main contributors to the folding of structured proteins, giving rise to compact tertiary structures. Consequently, bulky and hydrophobic amino acids are rare in IDRs [11]. Also, disordered regions often show a high net charge. The electrostatic repulsion between charges within the IDRs leads to more extended conformations than seen in structured regions [15].

The properties of IDRs offer advantages in several cellular processes, including both DNA-protein and protein-protein interactions. IDRs often undergo a disorder-to-order transition upon binding to a target. In this process, the disordered region folds into an ordered structure, which leads to a considerable decrease in entropy. However, the loss is compensated for by a favorable enthalpic gain. These interactions often show high specificity and low affinity. Thus, they are essential in signaling processes where the proteins involved should be able to bind to a specific target and dissociate quickly when the signaling is complete. Also, IDRs are frequently targeted in post-translational modifications (PTMs), where the range of protein functions is increased by modifying the polypeptide chain. PTMs include modulation of the chemical nature of amino acids, the addition of functional groups or peptides, and cleaving of the protein backbone. The flexibility and disorder of IDRs make them more accessible to the modifying enzymes since the side chains are more exposed than in structured regions [6, 10].

The molecular mechanisms of IDPs and IDRs and their structure-function relationship are still not fully understood. Due to their involvement in many critical cellular processes,

IDPs are often associated with diseases, such as Alzheimer's and Huntington's disease. In these diseases, the pathological effects originate from mutations leading to changes in protein conformation. The effects of mutations are well-known in structured proteins, including misfolding and loss-of-function. However, the effects are not that well-understood in the disordered regions and remain to be discovered. The understanding of the physical mechanisms behind IDPs is crucial for the development of drugs targeting IDRs/IDPs and in the engineering of therapeutic IDRs/IDPs [1].

2.2 DNA

Deoxyribonucleic acid (DNA) is a double-stranded nucleic acid responsible for storing genetic information in cells. DNA consists of nucleotides, which are monomeric units composed of a five-carbon sugar, a phosphate group, and an aromatic base. The four aromatic bases present in DNA are thymine(T), cytosine(C), adenine(A), and guanine(G), and their arrangement determines the genetic code. The two complementary strands of DNA twist around each other forming a double helix, where each base in one strand matches and forms hydrogen bonds with one specific base in the other strand. The two bases must complement each other, giving the only pairing possibilities: A paired with T, and G paired with C [3].

2.2.1 DNA-protein interactions

The interactions between DNA and proteins are highly important for a large number of cellular activities, such as DNA transcription, replication, recombination and repair [3]. Proteins are crucial in the compaction of DNA inside the nucleus. The total length of human DNA is almost 2 m, while the size of the nucleus is limited to a few micrometers. Thus, the volume of DNA needs to be decreased drastically and the strands are therefore packed into highly ordered structures, known as chromatin [16]. These structures are formed when DNA twists around small proteins, called histones. These proteins contain high amounts of the positively charged amino acids lysine and arginine, and the binding between histones and DNA is therefore dominated by electrostatic interactions [3].

The human genome is composed of approximately 3 billion base pairs encoding 20,000

to 25,000 genes, and sequence-specific DNA-binding proteins must therefore be able to find the correct binding sites out of a gigantic number of potential sites in the DNA [17, 18]. Transcription factors (TFs) are examples of DNA-binding proteins, and their main cell function is to initiate, enhance, or inhibit the transcription of genes [3]. The large size of the human genome rises the question on how TFs and other DNA-binding proteins are able to efficiently find their target sequence.

A key feature of the DNA sequences, making them recognizable for the DNA-binding proteins, is their chemical surface signature. Each base pair has their own set of functional groups, and the combination of several base pairs stacked together gives rise to a recognizable pattern. The DNA-binding domains (DBDs) of the DNA-binding proteins will bind with greater affinity to DNA sequences that are complementary to their own surface. The double-helical structure of the DNA results in so-called major and minor grooves, where these patterns are exposed. The DBDs may bind to both major and minor grooves of DNA, but the binding is most often seen in the major groove due to more available space and opportunities for interactions. The binding is mediated by different types of interactions, including hydrogen bonds and electrostatic interactions. In addition, the phosphate groups present in the DNA backbone are negatively charged and interact with the positively charged amino acids in the binding proteins [3, 18, 19]. The hydrophobic effect is also an important driving force behind the formation of the DNA-protein complexes [20].

Normanno et al. [21] studied the search dynamics of DNA-binding proteins in mammalian cells. The authors discovered that the proteins search the nucleus by diffusion and transient binding to non-specific DNA, that is, not to their target sequence. However, this binding is inefficient. The authors suggest that this is due to competition from other DNA-binding proteins, both specifically or non-specifically bound to the DNA. When the DNA is bound to other proteins, its accessibility to the DNA-binding protein, searching for its target, decreases [21].

Non-specific interactions involve a general affinity of the protein for the DNA strand. This mainly includes the electrostatic interactions between the protein and the sugar-phosphate backbone of the DNA. For many DNA-binding proteins, the nonspecific binding may be viewed as an intermediate step followed by the site-specific target search. However,

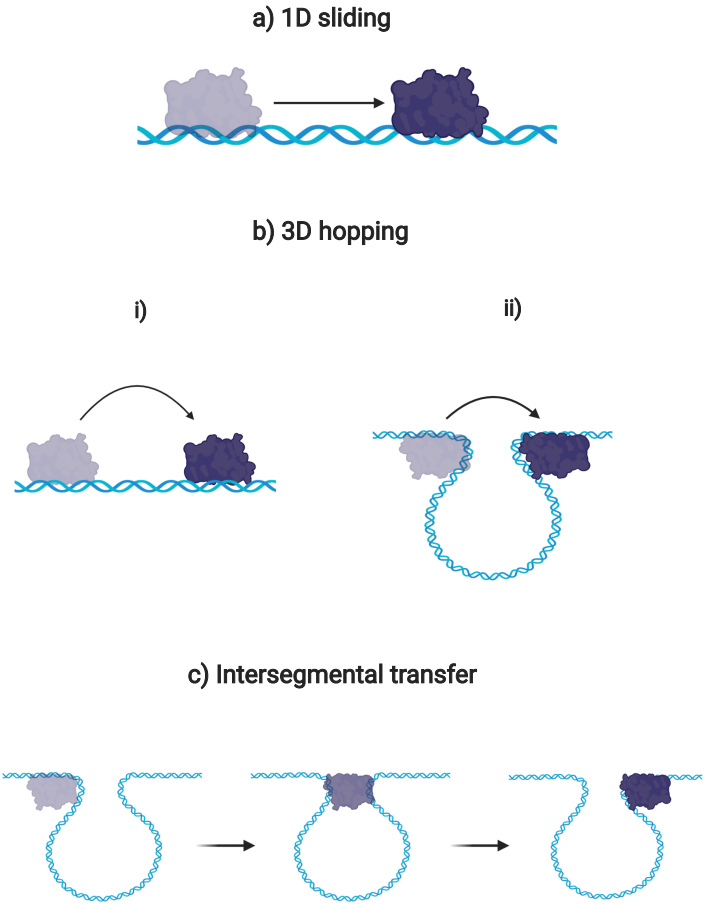

Figure 2.2: Facilitated diffusion of proteins along the DNA. Three mechanisms are shown, including (a) 1D sliding, (b) 3D hopping, and (c) intersegmental transfer. The mechanisms are shown for non-compacted, "naked" DNA, in contrast to the more compacted DNA found in the nucleus. Created with BioRender.com

not all DNA-binding proteins are site-specific, and they only bind DNA non-specifically [22, 23].

Facilitated diffusion describes the site-specific target search, and includes different actions, see Figure 2.2. 1D sliding refers to "sliding" of a protein along the DNA chain until it finds its target. Another mechanism is the 3D hopping, where the protein "jumps" from one segment to another. This usually occurs along the same DNA chain, but the protein may in some occasions move to another DNA molecule. The third mechanism is intersegmental transfer. Here, the protein binds to and brings two separate DNA fragments together via an intermediate loop. This is only relevant for proteins containing two DBDs, due to the binding of two DNA sites at the same time [24, 25].

2.2.2 Disordered regions in DNA-protein interactions

As mentioned in Chapter 1, many DNA-binding proteins contain disordered regions, such as disordered tails and flexible linkers. Several studies show that the amino acid composition of these regions plays an important role in protein-DNA interactions.

Gao et al. [26] studied the interactions between DNA and H-NS proteins. H-NS is a nucleoid-associated protein (NAP), which is a class of proteins involved in the packing and organization of DNA in bacterial cells. H-NS is known for its role in gene regulation in bacterial genomes, and consists of an N-terminal oligomerization domain and a C-terminal DNA binding domain, connected by a flexible linker. Gao and co-authors discovered that the number of positively charged residues greatly affect the electrostatic interactions between the linker and DNA molecule. These interactions contribute to a fast initial binding, and may also allow H-NS to perform 1D sliding along the DNA to find its specific binding site. Deletion of the whole linker or reduction in the number of positively charged residues lead to a drastic decrease in binding between H-NS and DNA. This indicates that the binding affinity strongly depends on the existence and the composition of a linker region [26].

Another study was performed by Subekti et al.[5], where the function of the flexible linker in the tumor suppressor p53 was evaluated. p53 is a crucial transcription factor in the maintenance of genomic integrity. Around 50% of cancer cells in humans have mutations in the p53 gene [7], and the p53 protein is therefore widely studied. p53 is activated when cells are exposed to various types of stresses, participating in the regulation of several processes, such as DNA repair, apoptosis, and cell cycle arrest [27]. Following the nonspecific binding of protein to DNA, the protein searches among large amounts of DNA before it finds and binds to its specific target sequence. The binding leads to the expression of proteins needed for the regulation of the mentioned processes. p53 binds to DNA and searches for its target sequence by facilitated diffusion, including both 1D sliding and 3D hopping [5, 28]. Several studies have investigated the binding due to the DBDs of p53 [29, 30], while the impact of the flexible linker still needs further investigation [5]. However, Subekti et al. revealed the importance of the p53 linker composition in both 1D sliding and the nonspecific DNA-binding. The disordered flexible linker of p53 possesses five positively charged amino acids. In their study, different variants of p53 with

modulated charges were prepared. The results showed that the neutralization of linker charges lead to a decrease in the nonspecific binding to DNA. This indicates that the linker directly interacts with the DNA, which may include the electrostatic interactions between the positively charged linker residues and the negatively charged DNA backbone. Furthermore, the neutralization promoted 1D sliding along the DNA, suggesting that the charge also regulates the 1D sliding dynamics. The conservation of linker residues between different mammals was also investigated, showing that the positively charged residues were highly conserved between species. This also supports the importance of these amino acids in the interaction between p53 and DNA.

Levy et al. [4] studied the disordered tails of p53. Disordered tails of DNA-binding proteins often show a high number of positive charges clustered together. The tails may facilitate DNA-binding via a "monkey bar" mechanism, which resembles the motion of a child swinging from one monkey bar to another. The tail can in the same way promote intersegmental transfer for a DNA-binding protein by "swinging" to a DNA strand, while the protein is still bound to another DNA strand. The p53 protein has an N-terminal and a C-terminal tail, which are negatively and positively charged, respectively. Consequently, the C-tail is of most interest in the protein-DNA interaction, due to its possibility of interacting with negatively charged DNA. To study the effect of the C-tail composition on the motion along DNA, the authors made different variants of the C-tail. They found that a higher number of intersegmental transfers occurred when the charges were clustered together and when the tail was significantly but moderately charged. This indicated that both the net charge and the position of the charges affected the "monkey bar" mechanism and hence influence the DNA search by DNA-binding proteins.

2.3 PAMAM dendrimers

Dendrimers are polymeric molecules consisting of tree-like arms or branches, and are known for being well-defined, homogenous in structure, and monodisperse in size. The molecules are made up of three main parts, including (1) a multifunctional core, acting as an anchor point for the branches, (2) inner branches, and (3) exposed terminal functionalized branches on the surface. Each layer of the inner branches makes up a generation,

adding exponentially more branching points for each additional layer. The functionality of the terminal branches can be modified in different ways, including the covalent binding of small molecules, drugs, and biomolecules, thereby changing the properties of the dendrimers. Dendrimers have a wide field of applications, including drug delivery, gene delivery, diagnostics, and vaccines [31, 32].

Poly(amidoamine)(PAMAM) dendrimers are the most well-studied and commercially available class of dendrimers. They are made up of a large number of amine and amide functional groups, which makes them highly suitable for biological applications [32]. Figure 2.3 shows a PAMAM dendrimer of generation 2 (G2) with an ethylenediamine core and 16 amine groups exposed on the surface. These outer groups are primary amines, while the interior amines are tertiary. The protonation of the amine groups, hence the addition of a positive charge, is highly dependent on pH [33]. However, all primary amine groups are protonated at pH 7.5 [34].

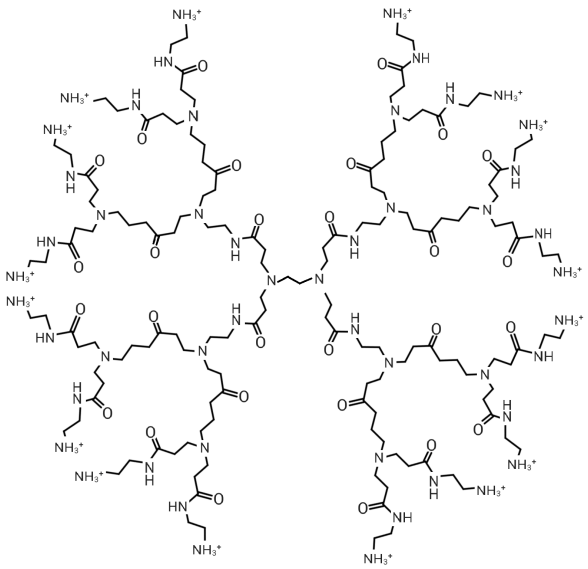

Figure 2.3: PAMAM generation 2 dendrimer (G2) with an ethylenediamine core and 16 protonated endgroups.

2.3.1 DNA condensation by PAMAM dendrimers

PAMAM dendrimers may be used as histone mimicking agents, because of the possibility of tuning both their size and surface charge density. In simple models, they are useful in

studying condensation and DNA-macromolecule complex formation, as well as how the complex structure influences the biological function of DNA. When in a buffer solution, the DNA strands adopt the conformation of semiflexible coils. However, when PAMAM dendrimers are added to the solution, electrostatic interactions between the anionic DNA backbone and cationic dendrimers lead to a more compact DNA conformation. This process is known as DNA condensation. The degree of condensation upon binding is dependent on both the dendrimer generation and the charge ratio, i.e. the ratio between positive amines on the dendrimers (NH_3^+) and negative phosphates on the DNA (PO_4^-) [35, 36].

There are several factors controlling the interactions between charged polymers, such as DNA and PAMAM. In solution, each polymer is surrounded by oppositely charged ions, known as counterions, which form a diffuse layer around the polymer [37].

The association of DNA and dendrimer results in the release of counterions from both species into solution, which leads to a large increase in mixing entropy. Consequently, the association is mostly entropically driven [16]. Further, due to the large charge of the dendrimers, these will correlate along the DNA chain and induce attractive interactions between DNA chains [38], leading to their condensation. However, there are also opposing forces, such as the loss of configurational entropy of the DNA molecule. The entropy loss is due to the decrease in volume occupied by the DNA molecule upon condensation. Also, the condensation leads to an increase in bending of the DNA, which brings the different parts of the molecule closer, and potentially increasing the intramolecular electrostatic repulsion, if the complexes are not neutral [39].

Previous studies have shown that the complex formation between DNA and PAMAM dendrimers is a cooperative process, resulting in a coexistence of both free and compacted DNA molecules, where dendrimers prefer to bind to an already partially compacted DNA, rather than to free DNA molecules. This cooperative binding is due to the strong attractive ion correlation effect [36, 39], as discussed above. The aggregates formed depend on the PAMAM dendrimer generation. Lower generation (1-2) dendrimers tend to form well-structured rods and toroidal complexes, while higher generations are more likely to induce the formation of globular and less defined structures [16].

Chapter 3

Methods

3.1 Fluorescence spectroscopy

Luminescence is the light emitted from a substance after the absorption of energy to an excited state. The term may be divided into two, namely fluorescence and phosphorescence [40]. When a molecule absorbs a quantum of energy matching the difference between its energy levels, one of the electrons may transition from the ground state to an excited state of higher energy. Molecules are often raised to a higher vibrational energy level of an excited electronic state, and may relax to a lower vibrational state before emission of a photon. This is known as vibrational relaxation. Consequently, the molecule emits a photon of lower energy than the exciting photon [3, 41]. Fluorescence occurs when an electron transitions from an excited singlet state to the ground state, while phosphorescence refers to the electron returning to the ground state from a triplet excited state. The absorption and emission of light may be visualized by a Jablonski diagram, shown in Figure 3.1. The ground state, and first and second excited states are named S_0, S_1 and S_2, respectively. Within these electronic levels, the molecule can exist in different vibrational levels, given as 0, 1, 2, etc [40]. In addition, several other non-radiative processes may occur after the excitation, such as the vibrational relaxation, internal conversion and intersystem crossing. Internal conversion refers to the transition between electronic states, for example from S_2 to S_1. Intersystem crossing describes the forbidden transition from a singlet state to a triplet state, as for example S_1 to T_1, and may be followed by the emission of a photon, namely phosphorescence [41].

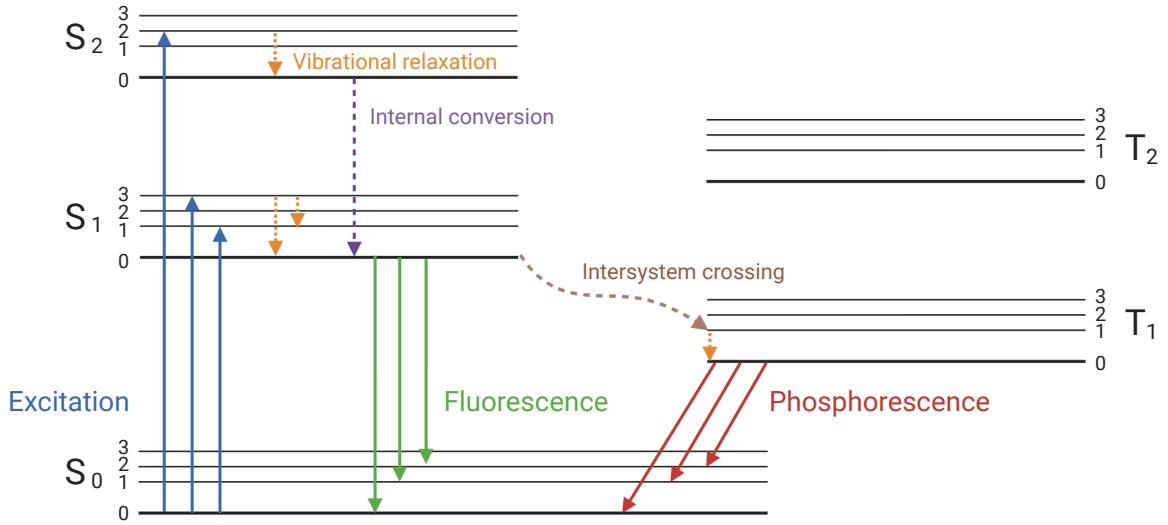

Figure 3.1: Jablonski diagram showing the transitions between states in a molecule after excitation by a photon. Electromagnetic radiation is emitted by fluorescence or phosphorescence, and they are visualized in the diagram as solid lines. Energy may also be lost in non-radiative processes, such as vibrational relaxation, internal conversion, and intersystem crossing, shown as dashed lines.

Fluorescence spectroscopy is a useful tool in investigating the interaction between PAMAM dendrimers and DNA. GelStar is a DNA binding dye known for being highly sensitive in the detection of nucleic acids. The fluorescence is greatly enhanced when the dye is bound to DNA, and the background fluorescence is negligible when DNA is absent. The stain has an excitation and emission maximum wavelength at $\lambda_{ex} = 493$ nm and $\lambda_{ex} = 527$ nm, respectively. When the DNA becomes more condensed, due to the presence of dendrimers, the dye is excluded from the DNA and the emission spectra is expected to show a lower fluorescence emission intensity than for the corresponding concentration of free DNA without dendrimers [35].

3.2 UV/Vis spectroscopy

Several biological molecules have specific absorbance in the UV/Vis region of the light spectrum, making it possible to determine their presence and concentration in solution. As mentioned, transitions between electronic states can occur when molecules absorb energy of photons. Molecules capable of absorbing UV/Visible light are known as chromophores, and their spectra are obtained by shining light of varying wavelengths through the sample and recording the intensity of the transmitted light. The Beer-Lambert law quantifies the absorption of light passing through a solution, and shows that the absorption is proportional to the concentration of chromophores [42]. The differential Beer-Lambert law is given by [43],

$$\frac{dI'}{dx} = -\epsilon c I' \tag{3.1}$$

where I' is light intensity and x is the dimension in which the light travels. ϵ refers to the molar absorptivity and has the SI unit of $\mathrm{m^2 mol^{-1}}$. c is the chromophore concentration. When the sample is placed in a cell of path length l, the equation may be written as,

$$\int_{I_0}^{I} \frac{dI'}{I'} = -\epsilon c \int_0^l dx \tag{3.2}$$

Here, the intensities of the light entering and exiting the solution are given as I_0 and I, respectively. The Beer-Lambert law defines the dimensionless absorbance A as,

$$A \equiv \ln \frac{I_0}{I} = \epsilon c l, \tag{3.3}$$

assuming a constant and uniform chromophore concentration c. The ratio between incoming and transmitted light is defined as the transmittance T,

$$T \equiv \frac{I}{I_0} = e^{-\epsilon c l}. \tag{3.4}$$

3.3 Gel electrophoresis

Gel electrophoresis is a technique used to separate charged molecules in an applied electric field. When charged biomolecules are placed in an electric field, they migrate towards the electrode of opposite charge due to electrostatic forces. The migration of the molecules depends on several factors, including charge/mass ratio, net charge and molecular shape [44]. A charged particle in an electrical field will experience a force described by Coulomb's law [45],

$$F = ZeE, \tag{3.5}$$

where Z corresponds valency of the species, e is the elementary charge, and E is the electrical field given in potential per cm. The particle will resist motion by $-fv$, where f is the frictional factor and v is the velocity of the particle. It is assumed that the net force on the particle in steady motion is zero, which gives

$$fv = ZeE. \tag{3.6}$$

The ratio between velocity and the strength of the electrical field is defined as the electrophoretic mobility U, which may be expressed as

$$U = \frac{v}{E} = \frac{Ze}{f}. \tag{3.7}$$

The movement of macromolecules depends on the substance in which they travel in. A gel with a given concentration may be viewed as a molecular sieve, in which the molecules under study move with more constraints compared to in solution. In DNA, the charge is proportional to its length. This implies that the electrophoretic mobility in solution becomes nearly independent of the molecular weight. In a gel, the molecules are therefore separated based on their ability to penetrate and reptate through the gel. That is, they are separated based on their molecular size. The size of an unknown DNA molecule may be determined by comparing it to a series of fragments with known molecular weights, the so-called ladders [45].

In this study, gel electrophoresis was used to assess the interactions between DNA

and PAMAM or PAMAM-peptides. Upon binding, the electrophoretic mobility may change due to several factors. The addition of positively charged molecules and complex formation, neutralize the negative charges in the DNA backbone, leading to a decrease in the mobility. In addition, the formation of large complexes increases the molecular weight and size, also reducing the mobility [46].

3.4 Mass spectrometry

Mass spectrometry is an analytical technique used to determine the mass of molecules. The technique has high sensitivity and is widely used in chemistry and biological sciences, for example characterization and identification of macromolecules and proteins [47]. The basic principle of mass spectrometry is the generation of ions in gas phase, followed by their separation and detection based on mass-to-charge ratio (m/z). A mass spectrometer generally consists of an ion source, a mass analyzer and a detector in high vacuum. The results are given as the signal intensity as a function of the m/z ratio [48].

In this study, mass spectrometry with electrospray ionization (ESI) was used to characterize PAMAM-peptide conjugates. ESI is a soft ionization method with nearly no fragmentation upon ionization, and the molecules are often ionized with multiple charging. Due to the higher number of charges per molecule, the m/z values become lower and the ratio may therefore be found in the range of the mass analyzer. Thus, ESI is often used in the study of large biological macromolecules, such as proteins and nucleic acids, due to the possibility of multiple charging [49].

When PAMAM dendrimers are ionized in ESI, they may be described in the form $[M+zH]^{z+}$, where M is the molecular mass, H is a hydrogen atom and z defines the charge state. The signals of the protonation states may be observed in the mass spectrum at ratios

$$\frac{m}{z} = \frac{M + zm_H}{z}, \tag{3.8}$$

where M corresponds to the mass of the molecule and m_H is the proton mass. It should be mentioned that other molecules apart from hydrogen, such as sodium (Na^+), can ionize the molecules of interest in mass spectrometry [50]. However, the protonation by hydrogen atoms was most relevant in this study due to the experimental setup, which will not be

described in detail here.

ESI, together with the high resolution mass spec system, makes it possible to determine the charge state of a given molecule by looking at the spacing between the peaks of an isotopic cluster. The cluster appears as a distribution of peaks in the mass spectrum, due to the different isotopes of the elements composing the molecule [50, 51]. An example is shown in Figure 3.2.

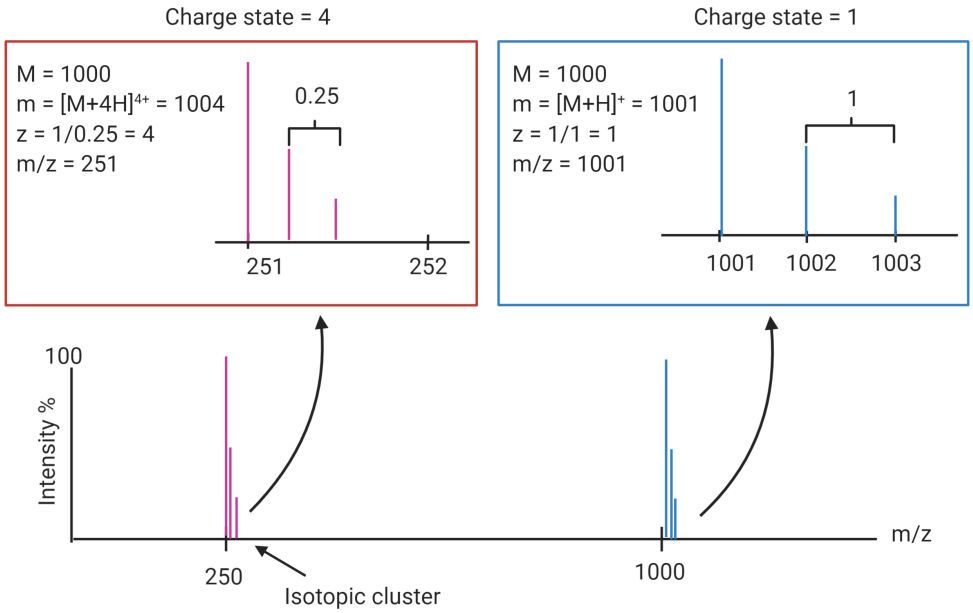

Figure 3.2: A simplified mass spectrum showing the isotopic clusters at charge states 1 and 4 for a molecule of molecular mass 1000 Da.

Chapter 4

Experimental procedures

4.1 Materials and sample preparations

4.1.1 DNA

10 mg/mL salmon sperm DNA (under 2 kbp) was received from Invitrogen. The Oct-1 DNA plasmid (3605 bp) was obtained from Integrated DNA Technologies (IDT). Stock solutions were prepared using PBS-EDTA buffer (10mM PBS, 1 mM EDTA, pH 7.4).

4.1.2 PAMAM dendrimers

20 wt.% PAMAM dendrimers generation 2.0, with ethylenediamine cores, were received in methanol solution from Sigma-Aldrich. To exchange the methanol with PBS-EDTA buffer (10mM PBS, 1 mM EDTA, pH 7.4), a dialysis was performed using dialysis tubes from the Pur-A-Lyzer Mega Dialysis Kit, delivered by Sigma-Adrich, with MWCO of 1 kDa. The capacity of the tubes was 3-20 mL, therefore, 400 μL of PAMAM solution was diluted in 3600 μL buffer prior to the dialysis. In accordance with the kit instructions, the following procedure was performed. First, the Pur-A-Lyzer tube was filled with ultrapure water, incubated for 5 minutes, and emptied. The diluted sample was loaded into the tube and placed in the supplied floating rack in a beaker containing 800 mL of PBS-EDTA buffer. It was left to stir for 7 hours. The buffer was then exchanged with 500 mL new buffer and stirred at low speed overnight. The following day, the sample was transferred from the Pur-A-Lyzer into a clean eppendorf tube.

4.1.3 Peptide sequences

The peptide sequences were designed by Corinna Dannert, and possessed different overall charge, charge distribution and density, in order to investigate the impact of these parameters on DNA-binding. The custom made peptides were produced and delivered by GenScript, and Figure 4.1 shows the amino acid sequences. The properties of the peptides, including length, overall charge, amino acid composition and purity, are shown in Table 4.1. All peptides contained a cysteine residue in each end. This was required for their conjugation to PAMAM dendrimes, as discussed in detail below. The peptides, delivered lyophilized, were solubilized in PBS buffer (0.5 M NaCl, 10% glycerol, pH 7.4). Most of the peptides were easily dissolved in 200 μL buffer. However, peptides SN8-24 and N-end-25 required additional heating to dissolve, and their tubes were heated in a water bath with a temperature of approximately 65°C. Aliquots were made for each peptide and stored at -85°C. peptide S-25 was dissolved before the start of the project in Tris-HCl (10 mM, pH 7.4).

Table 4.1: Properties of the studied peptide sequences, including polymerization number, overall charge, and amino acid composition.

Name	Polymerization number	Overall charge	M_w (Da)	Amino acids
S-25	27	0	2042	Serine, Glycine
SP-25	27	+12	2895	Serine, Lysine(+)
NP-25	27	-1	3259	Aspartic acid(-), Lysine(+)
N-end-25	27	-8	2386	Serine, Glycine, Aspartic acid(-)
P-end-25	27	+8	2491	Serine, Glycine, Lysine(+)
N-mid-24	26	-8	2299	Serine, Glycine, Aspartic acid(-)
P-mid-24	26	+8	2403	Serine, Glycine, Lysine(+)
SN8-24	26	-8	2329	Serine, Glycine, Aspartic acid(-)
SP8-24	26	+8	2433	Serine, Glycine, Lysine(+)

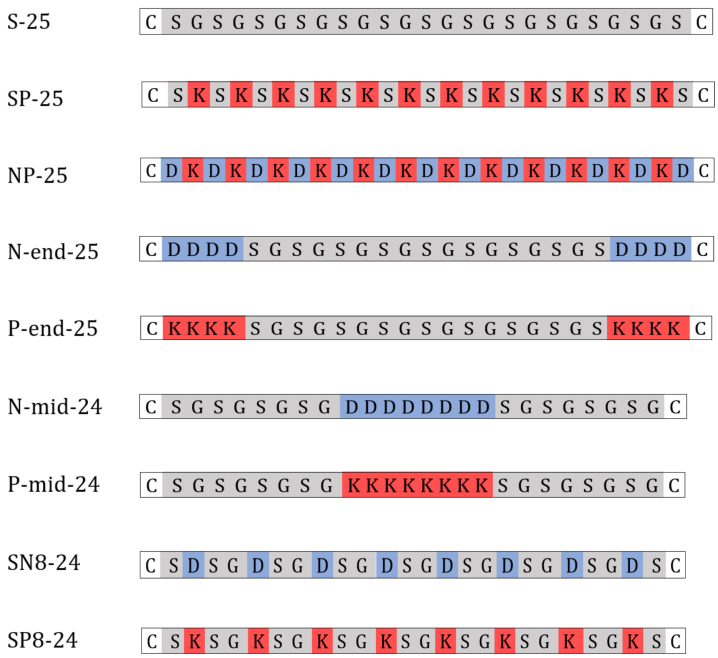

Figure 4.1: Peptide sequences conjugated to PAMAM dendrimers. The letters are abbreviations for the amino acids composing each peptide, namely cysteine(C), serine(S), glycine(G), aspartic acid(D), and lysine(K). The colors indicate their side chain charge, where red, blue and grey are positive, negative and neutral charge, respectively.

4.1.4 Other materials

Phosphate buffered saline (PBS) tablets and ethylenediaminetetraacetic acid (EDTA) for buffer preparation were purchased from Sigma Aldrich. DTT and Sulfo-LC-SPDP, used in the conjugation procedure, were also aquired from Sigma-Aldrich. PlusOne Mini Dialysis Kit was used in the dialysis of the conjugated samples and was delivered by GE Healthcare. PageBlue Protein Staining Solution, used in the assessment of conjugates, was obtained from Thermo Scientific. Vivacon 500 concentration tubes, with a MWCO of 2 kDa, were delivered by Sartoius. GelStar x10 000 was used in dye exclusion assays and gel electrophoresis and purchased from Lonza. Etidium bromide, also used in dye exclusion assays, was received from Sigma-Aldrich. 10x TBE electrophoresis buffer and 6x Tri-track DNA loading were purchased from Thermo Fisher Scientific. 10x TAE buffer and Agarose were delivered by Millipore and Sigma-Aldrich, respectively.

4.2 Conjugation of PAMAM dendrimers and peptides

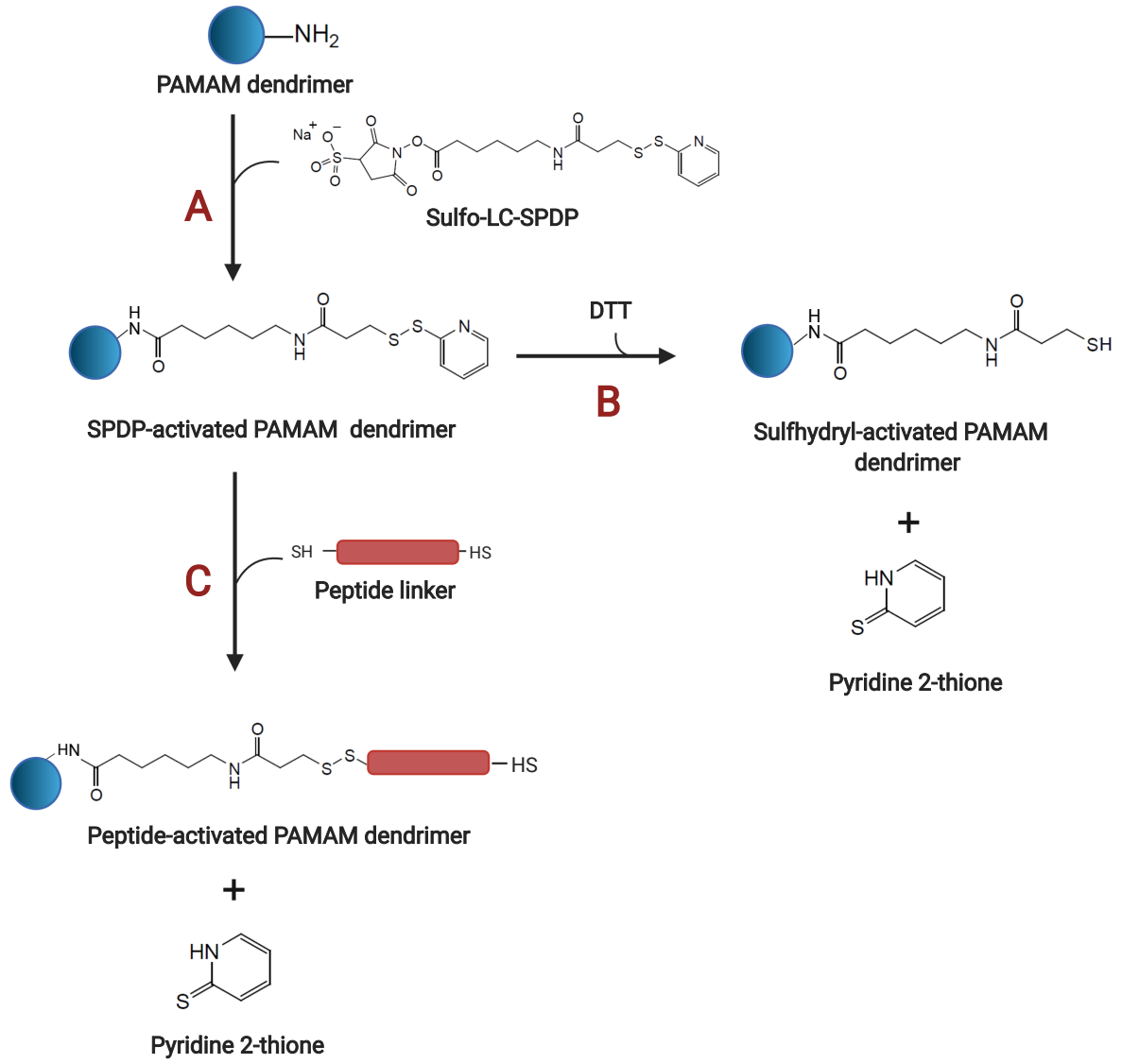

Figure 4.2: Reactions involved in the conjugation of PAMAM dendrimers to peptides. Reaction A shows the attachment of crosslinkers to dendrimers. This reaction is followed by a dialysis to remove the unreacted crosslinkers. The number of crosslinkers successfully connected to the dendrimers is assessed by adding dithiothreitol (DTT) to the solution (Reaction B) and measuring the absorbance of the resulting pyridine 2-thione at 343 nm. In Reaction C, peptides are mixed with SPDP-activated PAMAM dendrimers. This reaction also releases pyridine 2-thione, and the extent of the reaction is also assessed by measuring the absorbance of the reaction solution at 343 nm. Redrawn from Santos et al. [52]. Created with BioRender.com.

Figure 4.2 shows the reactions involved in the conjugation of the peptides to the PAMAM dendrimers. The conjugation procedure is based on the experiments performed by Santos et al. [52] and Waite et al. [53].

Crosslinkers are firstly bound to amine groups on the dendrimer surface (Reaction A). To assess the average number of crosslinkers bound to the dendrimers, the disulfide bond present in the crosslinkers may be cleaved by dithiothreitol (DTT) (Reaction B). The reaction releases a pyridine-2-thione group, which has an UV absorbance at 343 nm, making it possible to quantify the average number of crosslinkers attached, using UV/Vis spectrophotometry [54].

The crosslinkers allow for the attachment of peptides (Reaction C). The peptides are all cysteine-modified in each end, which enables the formation of a disulfide bridge between the crosslinker and peptide. N-succinimidyl 3-(2-pyridyldithio) propionate (SPDP) reagents belong to the class of amine- and sulfhydryl-reactive heterobifunctional crosslinkers, and they are used in both amine-to-amine or amine-to-sulfhydryl crosslinking. Crosslinking with SPDP is often used in the conjugation of proteins. However, it is not limited to experiments involving proteins. The procedure requires that the reacting molecules contain primary amines (-NH_2) or sulfhydryl groups, which includes a variety of other types of molecules. The PAMAM G2 dendrimers display 16 amine groups on their surface, and are therefore well-suited targets for the SPDP reagent. The part of SPDP that reacts with amines is the N-hydroxysuccinimide(NHS) ester, see Figure 4.2. Different types of SPDP reagents may be used, including SPDP, LC-SPDP, and Sulfo-LC-SPDP. They vary in molecular weight and structure, in addition to water solubility, where the Sulfo-LC-SPDP is the only one that is water-soluble [54]. Thus, it may be added directly to aqueous solutions and is therefore chosen as crosslinker in this project. It will be further referred to as SPDP. Pyridine-2-thione is also released when the peptides are conjugated to the crosslinkers on the dendrimers (Reaction C), and the absorbance of the solution may again be used to assess the reaction yield [52].

4.2.1 PAMAM-SPDP-peptide conjugation

The experimental procedures behind the reactions shown in Figure 4.2 are described in detail in this section.

Conjugation of PAMAM dendrimers and SPDP crosslinkers (Reaction A)

A 3.88 mM dialyzed PAMAM stock solution (in PBS-EDTA buffer) was diluted with PBS-EDTA buffer to achieve a concentration of 0.1 mM. The final volume varied between batches. Sulfo-LC-SPDP, with a concentration of 50 g/L, was added to the PAMAM solution to achieve the desired SPDP:PAMAM molar ratio. This implies, for example, that 6 SPDP molecules are added per PAMAM dendrimer if the molar ratio is 6. The solution was left to stir for 2.5 hours at room temperature, before being transferred to a Pur-A-Lyzer Dialysis tube, with a MWCO of 1 kDa, and dialyzed in buffer overnight to remove any unreacted SPDP. The following day, the dialyzed PAMAM-SPDP solutions were weighed and transferred to eppendorf tubes.

The conjugation of PAMAM dendrimers and SPDP crosslinkers has been performed in several studies [52, 53]. However, the authors have primarily used dendrimers of higher generations than G2, such as G5. Thus, the SPDP:G2 to obtain a desirable number of covalently bound cross links had to be investigated. To determine a suitable amount of SPDP relative to PAMAM, four solutions of 4 mL with constant PAMAM (0.1 mM) and varying SPDP concentrations were prepared to give the final concentration of SPDP:PAMAM 3, 4, 5 and 6, see Table 4.2. 800 μL of the resulting solutions were dialyzed overnight against 2 L PBS-EDTA buffer.

A SPDP:PAMAM of 6 was found to give the desired conjugation, see Section 5.1.1, and two more batches were prepared. In the second batch, a 6 mL of 0.1 mM PAMAM was prepared, and a total amount of 3.6 μmol SPDP was added. The solution was divided into two solution of 3 mL before mixing, to ensure even mixing of PAMAM and SPDP. The two solutions were brought together and dialyzed in one dialysis tube. In contrast to the previous batch, the buffer volume was 800 μL and exchanged two times during dialysis, with time intervals of overnight, 5 hours and overnight.

In the third batch, a 10 mL solution of PAMAM-SPDP was made to allow the preparation of a 1 mL PAMAM-SPDP-peptide solution for all peptides. The 10 mL PA-

MAM solution was divided into four, and 6 μmol of SPDP was evenly mixed to a final SPDP:PAMAM of 6. The four solutions were afterwards mixed together and the resulting 10 mL solution was dialyzed against 1.5 L buffer overnight. The buffer was exchanged with 1 L and dialyzed for one more night.

Table 4.2: Molar ratios of Sulfo-LC-SPDP added to the 0.1 mM PAMAM solutions (Reaction A) in each batch. The SPDP corresponds to the amount (μmol) added per mL of PAMAM solution. The peptides conjugated to the PAMAM-SPDP complexes (Reaction C) are also shown for each batch. In the first batch, only solutions of molar ratios 3 and 6 were conjugated with the S-25 peptide.

Batch	Molar ratio (SPDP:PAMAM)	SPDP (μmol)	Conjugated peptide
1	3	0.3	S-25
	4	0.4	-
	5	0.5	-
	6	0.6	S-25
2	6	0.6	SN8-24
3	6	0.6	All peptides

Assessment of PAMAM-SPDP conjugation with DTT assay (Reaction B)

As in Waite et al. [53] and the protocol referred to in their study [54], the PAMAM-SPDP conjugate solutions were treated with DTT to assess the average number of SPDP conjugated to PAMAM. The absorbances were measured with an Agilent 8453 UV/Vis spectrophotometer. A stock solution of 15 mg/mL DTT was prepared in PBS-EDTA buffer. 100 μL of PAMAM-SPDP conjugates solution was mixed with 900 μL PBS-EDTA buffer. The absorbance of each sample was measured prior to the addition of DTT, giving the background absorbance. To each sample, 10 μL of DTT was added directly to the cuvette, mixed and left to equilibrate for exactly 15 minutes. The increase in absorbance after the addition of DTT was used to calculate the average number of SPDP conjugated to each dendrimer, according to,

$$\Delta\text{A343} = (\text{A343 after DTT}) - (\text{A343 before DTT}). \tag{4.1}$$

The molar ratios (SPDP:PAMAM) were calculated using,

$$\frac{\Delta \text{A343}}{8080} \cdot \frac{\text{M}_w \text{ of PAMAM}}{\text{c}_{\text{PAMAM}} \text{ in final solution (mg/mL)}} = \text{moles SPDP per mole of PAMAM,} \quad (4.2)$$

where the value 8080 is the extinction coefficient of pyridine-2-thione at 343 nm: $8.08 \cdot 10^3 \text{M}^{-1}\text{cm}^{-1}$.

Addition of peptides to PAMAM-SPDP conjugates (Reaction C)

Following the calculation of the average number of SPDP crosslinked to PAMAM, peptides were added to the PAMAM-SPDP solutions with a peptide:SPDP of 1. The solutions were left to mix overnight at room temperature. The conjugation was evaluated with a DTT assay the following day. The assay was performed in the same way as described in the previous section (Reaction B), where the absorbance of pyridine-2-thione at 343 nm was measured before and after the addition of DTT.

For Batch 3, an additional dialysis was performed after the addition of peptides, to remove the excess pyridine-2-thione released in the reaction. The dialysis was performed for all solutions, where 1 mL of each PAMAM-SPDP-peptide conjugate solution was dialyzed in PBS-EDTA buffer overnight with an additional change of buffer the next day. The PlusOne Mini Dialysis Kit from GE Healthcare was used, due to a more suitable volume range (200 μL-2 mL), compared to the Pur-A-lyzer tubes used previously. However, the dialysis tubes had the same MWCO (1 kDa). The dialysis was conducted according to the manufactures instructions. The dialysis tube and cap were rinsed with distilled water, and the cap was placed, with the membrane facing down, in a clean beaker containing distilled water. Directly before use, the cap was taken out from the beaker and the excess water was removed with a pipette. The PAMAM-SPDP-peptide solution was placed in the dialysis tube, before placing the cap and inverting the tube. The sample was ensured to be resting on the cap membrane and dialyzed on a floating rack overnight. The following day, the tube was centrifuged for 5-6 seconds at around 700g to collect the sample in the bottom of the tube, before transferring it to a clean eppendorf tube.

4.3 Characterization of PAMAM-peptide conjugates

For simplicity, the PAMAM-SPDP-peptide conjugates will here after be referred to as PAMAM-peptide conjugates.

4.3.1 Mass spectrometry

Mass spectrometry was used to investigate the molecular weight of the conjugation reaction products, and thereby verify the conjugation and characterize the resulting molecules. The instrument used was LC-ESI-qTOF-MS (positive resolution mode) with Acquity UPLC BEH300 C18 columns. The measurements were performed by Kåre Andre Kristiansen, who decided all experimental settings.

Three samples, containing PAMAM, SN8-24 peptides, and PAMAM-SN8-24, were prepared as described above and dialyzed in deionized water with 1 kDa MWCO dialysis tubes overnight. Afterwards, the PAMAM-SN8-24 solution was concentrated using concentration tubes with 2 kDa MWCO. The final concentration of the PAMAM, SN8-24, and PAMAM-SN8-24 solutions was approximately 0.8 mg/mL.

4.3.2 Agarose Gel electrophoresis and PageBlue Protein Staining

Agarose gel electrophoresis was performed in an attempt to characterize the PAMAM-peptide conjguates.

In the preparation of the agarose gel (5%), 5 g of Agarose was mixed with 100 mL of 1x TAE buffer. The solution was heated up to dissolve the agarose and left to cool. It was then transferred to a VWR casting tray and left to settle for 60 minutes. The gel was further placed in the electrophoresis chamber and covered with 1x TAE buffer. The samples studied were PAMAM, SP8-24 peptide, PAMAM-SP8-24 conjugate, SN8-24 peptide and PAMAM-SN8-24 conjugate. Three different concentrations were used for each solution, where the lowest concentration ranged from 0.05-0.1 μg, the middle ranged from 0.5-1 μg, and the highest ranged from 5-10 μg, depending on the sample. 10 μL of each solution was mixed with 2 μL of 6x Loading Dye, and 10 μL of the solutions were placed in each well. The gel were run for 20 minutes at 90 V. Afterwards, the gel was placed in a tray and PageBlue Staining dye was added to cover the gel. It was left for 2

hours, before being washed with water.

PageBlue has the same properties as the common Coomassie G-250 dye for protein staining, but has a 10 times higher sensitivity [55]. Coomassie Blue has been used to stain PAMAM dendrimers in previous studies, using either agarose [56] or polyacrylamide gels [57]. The exact mechanism behind Coomassie Blue staining of proteins and dendrimers is not fully understood, but it is believed to be due to interactions between the dye and the amine groups of the molecules to be stained [57].

4.4 Fluorescence spectroscopy

Fluorescence spectroscopy and dye exclusion assays were used to compare the interactions between DNA and the different PAMAM-peptide conjugates. The linear dependence of DNA concentration with fluorescence intensity was also confirmed.

4.4.1 Optimization of dye exclusion assay

Different protocols were tried to optimize the dye exclusion assay method for the systems studied. In general, the final concentrations of GelStar and DNA were kept constant at x10 and 2 μg/mL, respectively, while the concentration of PAMAM/PAMAM-peptides varied. All stock solutions were prepared with PBS-EDTA buffer, and all samples were made in triplicates. The changes done between protocols mainly involved the order and volumes used in the mixing of solutions.

In the first protocol, 60 μL of PBS-EDTA buffer, 10 μL of 20 μg/mL DNA and 10 μL of x100 GelStar were mixed in eppendorf tubes and left to equilibrate for 15 minutes. Afterwards, 20 μL of PAMAM dendrimers, with varying concentrations, were added. The samples were left to equilibrate for 30 minutes and then transferred to a BD Falcon 384 black well plate obtained from Thermo Fisher Scientific. A Spectramax I3X well scanner was used to measure the fluorescence emission intensity between 520 nm and 620 nm with intervals of 5 nm and an excitation wavelength of 493 nm.

In a second protocol, 20 μL of PAMAM were mixed with 10 μL of DNA and 60 μL PBS-EDTA buffer and left to equilibrate for 15 minutes. Afterwards, 10 μL of GelStar was added and left to equilibrate for 30 minutes before the samples were transferred and

measured as above.

The third protocol was inspired by Ainalem et al. [58], where DNA and PAMAM were mixed and allowed to equilibrate for a longer period of time before measurements. 45 μL of 4.44 μg/mL DNA, giving the same final DNA concentration as before, was mixed with 45 μL of PAMAM or PAMAM-peptide complexes of varying concentrations. The increase in volumes of the solutions being mixed eliminated the need for addition of buffer. In contrast to before, the samples were added directly and mixed in the well plate. The samples were left on mixing boards for approximately 2 hours, before adding 10 μL of x100 GelStar. The samples were left to equilibrate for another 30 minutes and measured as above. This protocol was chosen when comparing the interactions between DNA and different PAMAM-peptide complexes. In the optimization of protocols, salmon sperm DNA was used. The DNA was later changed to Oct-1, to improve the visualization of bands in gel electrophoresis (as discussed below), and used in all experiments involving DNA and PAMAM-peptide complexes.

A control sample, containing PAMAM-peptide complexes without DNA, was made in all experiments, to ensure that the complexes do not bind GelStar themselves. Control samples of peptides were also made, including samples containing peptide and GelStar with or without DNA. They were made to investigate if the peptide alone would bind to and condense DNA, and if the peptide alone would bind to GelStar.

The dye exclusion protocol was also attempted using Ethidium Bromide (EtBr) as dye, using the third protocol described above. Here, however, the 10 μL of x100 GelStar was exchanged with 10 μL of EtBr stock solution. The EtBr stock solution had a concentration of 12 μg/mL, giving a final concentration of 1.2 μg/mL. The final DNA concentration was 2 μg/mL. With the molecular weights of EtBr and DNA base being 394.3 Da and 330 Da in average, respectively, the concentrations used correspond to a ratio of one EtBr molecule per DNA base pair. The fluorescence emission intensity was measured between 550 nm and 650 nm with intervals of 5 nm and an excitation wavelength of 480 nm.

4.4.2 Relationship between DNA concentration and fluorescence intensity

To confirm that the used conditions were within the linear regime, the relationship between concentration of free DNA and fluorescence intensity was also investigated. The final concentration of GelStar was kept constant at x10 in all samples, while the final concentration of free DNA ranged from 0 to 4.9 μg/mL. All samples were made in triplicates. 10 μL of x100 GelStar was mixed with varying volume ratios of buffer and DNA stock solution to obtain the wanted final DNA concentrations. The final volume of the samples was 100 μL. The samples were left to equilibrate for 15 minutes, transferred to a plate and measured as described for GelStar.

4.5 Gel electrophoresis

Gel electrophoresis was used to investigate the degree of DNA condensation upon interaction with different PAMAM-peptide conjugates. The first experiments were performed using salmon sperm DNA, but this was later changed to Oct-1 binding DNA (not coding protein). The change was made because the bands in the gel are more distinct for Oct-1 DNA due to its monodispersity, when compared to the salmon sperm DNA used, which has a range of sizes, giving rise to a smeared band (see gels in Figures 5.14 and 5.15 in Section 5.4.1)

For the salmon sperm DNA, 1 g of Agarose was mixed with 100 mL of 1x TBE buffer. The solution was heated up to dissolve the agarose and left to cool before adding 5 μL of x10000 GelStar dye. It was then transferred to a VWR casting tray and left to settle for 60 minutes. The gel was afterwards placed in the electrophoresis chamber and covered with 1x TBE buffer. The final DNA concentration was 25 μg/mL in all samples with varying PAMAM concentrations. Equal volumes of DNA and PAMAM were mixed and left to equilibrate for 1 hour. 10 μL of each DNA-PAMAM solution was mixed with 2 μL of 6x Loading Dye, and 10 μL of the solutions were placed in each well. The gels were run for 50 minutes at 90 V. The DNA movements were visualized on a Benchtop 3UV Transilluminator at 302 nm.

For the experiments using Oct-1 DNA, 1x TAE buffer was used instead of 1x TBE.

In addition, the final DNA concentration was 10 μg/mL and the gels were run at 120 V for 40 minutes. The changes were made due to the good results obatined from previous experiments with the Oct-1 DNA performed by Corinna Dannert.

Chapter 5

Results and Discussion

5.1 Conjugation of PAMAM dendrimers and peptides

5.1.1 Conjugation of PAMAM dendrimers and SPDP crosslinker

The conjugation between PAMAM dendrimers and SPDP crosslinkers was investigated to determine an appropriate SPDP:PAMAM. Waite et al. [53] used the same DTT assay in quantifying the average number of SPDP conjugated to PAMAM G5 dendrimers. The authors used the theoretical molar ratios 6, 9, 12 and 15, in contrast to the 3, 4, 5 and 6, investigated in this study. The choice of ratios in this study was based on their results from the theoretical ratio of 6, where the average number of crosslinkers conjugated to dendrimers was 2.12. Since the main goal in this study was to achieve dendrimers with one or two tails, or dimers with a connecting peptide between two dendrimers, to mimic disordered tails and flexible linkers, this seemed like an appropriate maximum ratio to start with. Since the G5 dendrimers are significantly larger than G2, it was unclear if the conjugation would show the same results.

Figure 5.1 shows the results from the DTT assays performed in this study to estimate the number of SPDP conjugated to PAMAM. The light blue bars show the absorbance before the addition of DTT. This is the background absorbance and is close to zero for all solutions. The difference in absorbance before and after the addition of DTT corresponds to the amount of pyridine-2-thione in solution. The average number of crosslinkers conjugated to each dendrimer was calculated from Equation 4.2 for each of the SPDP:PAMAM

and is shown in Table 5.1.

From Figure 5.1a, it may be seen that the absorbance upon addition of DTT increases for increasing SPDP:PAMAM. This indicates that a larger number of SPDP covalently binds to PAMAM, when the concentration of SPDP is higher. The average number of SPDP conjugated per PAMAM increases from 1.47 to 2.56 when the molar ratio increases from 3 to 6. The same SPDP:PAMAM of 6 was used in two more batches, but the calculated molar ratios from these resulted in values of 2.17 and 2.34. Thus, they both gave a lower value than 2.56, but are still higher than the values for the theoretical molar ratios of 3, 4 and 5.

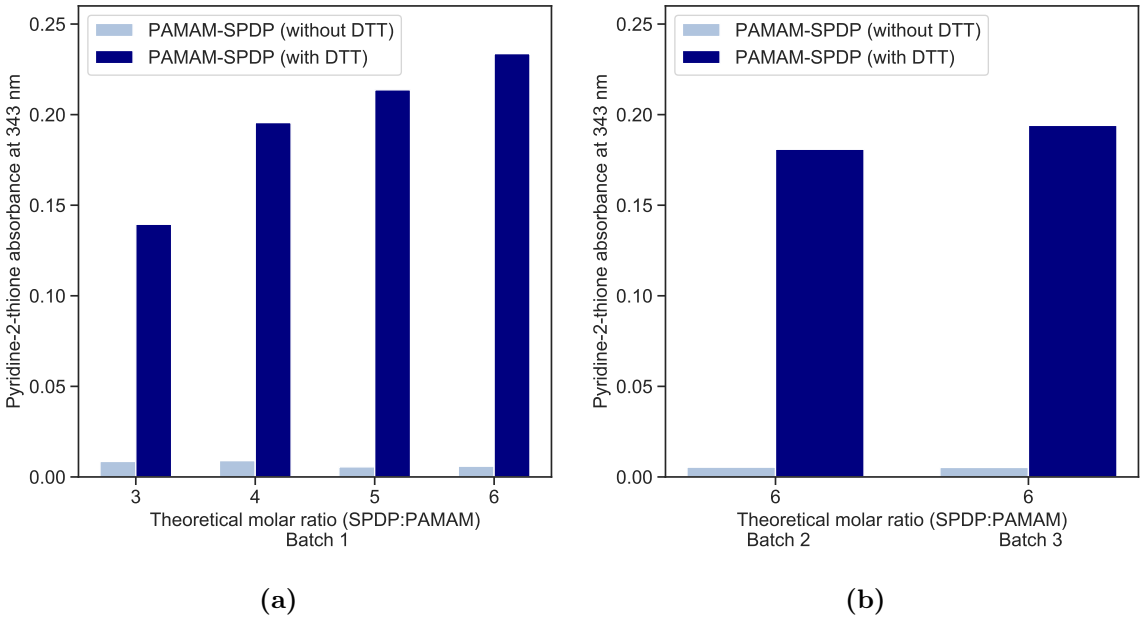

Figure 5.1: Absorbance of pyridine-2-thione measured at 343 nm for PAMAM-SPDP solutions before (background) and after the addition of DTT. Figure (a) shows the results for Batch 1, while Figure (b) shows for both batches 2 and 3. The theoretical SPDP:PAMAM are shown on the x-axes.

There might be several factors causing the differences in the experimentally determined ratios after DTT release for the same theoretical SPDP:PAMAM. For example, there might be some variations in the addition and mixing of DTT to the solutions before absorbance measurements. This may affect the reaction between DTT and PAMAM-SPDP, and therefore the absorbance. In addition, the dialysis time and buffer exchange was different the the three batches. If any free, non-conjugated SPDP molecules are present in solution, these will also be cleaved by DTT, contributing to the absorbance of

Table 5.1: Experimentally determined molar ratios (SPDP:PAMAM) for each of the theoretical molar ratios. The peptides conjugated in the following reactions are also shown for each batch.

Batch	Theoretical molar ratio	Experimental molar ratio by DTT release	Conjugated peptide
1	3	1.47	S-25
	4	2.10	-
	5	2.15	-
	6	2.56	S-25
2	6	2.17	SN8-24
3	6	2.34	All peptides

released pyridine-2-thione. Thus, the average number of SPDP attached to PAMAM will appear higher than the actual conjugation would have indicated.

To investigate if all unreacted SPDP is excluded from the samples during dialysis, a dialysis of SPDP alone was performed with a concentration corresponding to the one used in the SPDP:PAMAM of 6. Following the procedure in Batch 1, the buffer volume was not exchanged during dialysis. The absorbance of the non-dialyzed SPDP solution was 0.34, while that of the dialyzed was 0.07. Hence, not all SPDP left the dialysis tube, and some of the recorded absorbance in the samples may be affected by the non-reacted, free SPDP in solution. However, the buffer was exchanged during the dialysis procedures in batches 2 and 3, which might have made the potential error smaller, and could justify the decrease in absorption in batches 2 and 3.

It should also be noted that the resulting experimental ratios ranged from 2.17-2.56 for the PAMAM G2 dendrimers at an SPDP:PAMAM of 6, which are quite similar to the ratio of 2.12 determined by Waite and co-authors for the G5 dendrimers at the same SPDP:PAMAM.

5.1.2 Conjugation of PAMAM-SPDP complexes and peptides

Figures 5.2 and 5.3 show the absorbance at 343 nm of the PAMAM-peptide solutions before and after the addition of DTT. The absorbance before the addition of DTT, indicates a release of pyridine-2-thione due to the conjugation of peptides to PAMAM-SPDP (Reaction C). The increase in absorbance after DTT addition corresponds, in principle, to

the amount of remaining non-occupied SPDP crosslinkers. This is equivalent to Reaction B, but applied to the products of Reaction C. Consequently, if the absorbance is the same before and after the addition of DTT, one can assume that all SPDP crosslinkers are occupied by a peptide.

The peptides were added to the PAMAM-SPDP solutions with a peptide:SPDP of 1, based on the results obtained from the DTT assay. Naturally, if the average number of SPDP attached per PAMAM is deemed to be higher than it actually is, the real peptide:SPDP ratio in solution will also be higher than 1. However, the main goal of the following experiments is to investigate differences between peptides. Since the conjugates are prepared from the same batch this will not affect the comparison.

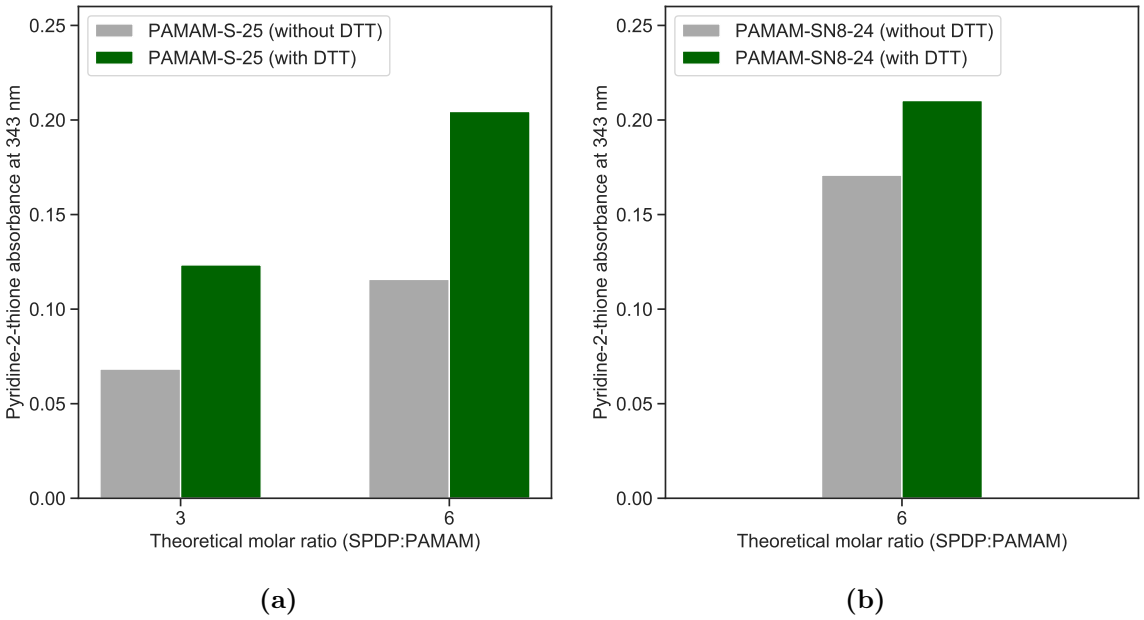

Figure 5.2: Absorbance of pyridine-2-thione measured at 343 nm for PAMAM-peptide solutions before and after addition of DTT for (a) Batch 1 with PAMAM-SPDP-S25 and (b) Batch 2 with PAMAM-SPDP-SN8-24.

In Batch 1, the neutral peptide S-25 was added to solutions with SPDP:PAMAM of 3 and 6. It may be seen from Figure 5.2a that around half of the final absorbance is present before the addition of DTT for both ratios. This suggests that half of the SPDPs on the dendrimers successfully conjugated with a peptide, while the other half did not. These results, and the ones shown for Batch 1 in the previous section, indicate that an added SPDP:PAMAM of 6 gives an average number of 2.56 SPDP per PAMAM, and half of

them are occupied by a peptide. Therefore, the SPDP:PAMAM ratio of 6 was chosen for batches 2 and 3, see Table 5.1, to increase the probability of one PAMAM having at least one conjugated peptide. In Batch 2, the negatively charged peptide SN8-24 was added to the PAMAM-SPDP solution, see Figure 5.2b. In this case, there seems to be a larger amount of crosslinkers reacting with the peptide, as compared to the previous batch.

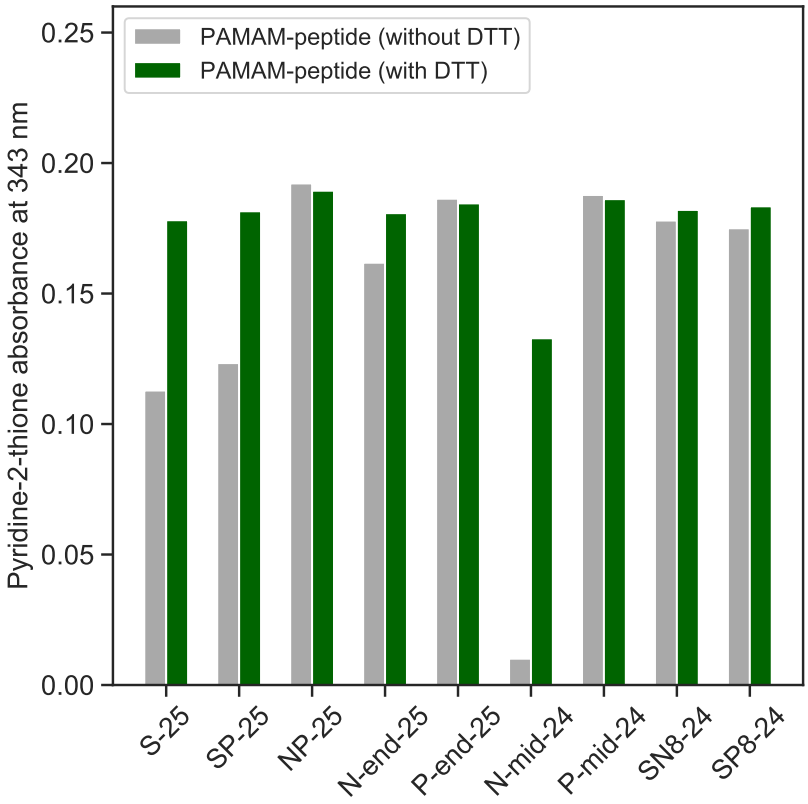

Figure 5.3: Absorbance of pyridine-2-thione measured at 343 nm for PAMAM-peptide solutions before and after addition of DTT for Batch 3.

Figure 5.3 shows the absorbance for the different PAMAM-peptide solutions in Batch 3. One could imagine that the positively charged peptides would show less binding to the positively charged PAMAM dendrimers compared to the neutral and negative peptides, as they repel in solution and can potentially limit their proximity, but this was not the case. However, there was still great variation in the yield for some of the reactions. For example, there is nearly no absorbance for the solution containing the N-mid-24 peptide before the addition of DTT, and the final absorbance is also remarkably lower than for the other solutions. The conjugation with this peptide was attempted again to investigate

if something went wrong during the first experiment. However, the second attempt gave the same results, and the peptide did not seem to conjugate at all. The reason for this is not clear, and the solution was not used in the later experiments.

For the SP-25, approximately two thirds of the absorbance is present before addition of DTT, indicating that two thirds of the crosslinkers are occupied with SP-25 peptides. For the other peptides, the bars show almost the same value before and after DTT addition, indicating that approximately all crosslinkers are occupied with peptides. The peptides are able to bind to SPDP in both ends of their sequences. Thus, there is a possibility that the molecules formed are dimers, where two PAMAM dendrimers are connected by one peptide linker. However, these experiments are not able to predict the structure of the resulting molecules, since they only tell if the SPDPs are occupied or not.

The results from the S-25 and SN8-24 conjugations in Batch 3 show approximately the same as the results in batches 1 and 2 for the same peptides. However, the absorbance before DTT addition is slightly higher for both peptides in Batch 3, indicating that the reaction yield is slightly higher.

Dialysis procedures were performed after both conjugation steps, namely after the PAMAM-SPDP and PAMAM-peptide conjugation. In the dialysis after PAMAM-SPDP conjugation, it is assumed that no PAMAM leaves the tube during dialysis, and that all PAMAM are extracted from the tube when the solution is transferred. The first assumption is probably valid, since the MWCO of the dialysis membrane is 1 kDa, and the molecular weight of PAMAM is 3256.18 Da. The second might be less valid, since some PAMAM may adsorb to the dialysis membrane, thereby changing the actual concentration in the final solution. Correction of concentration was performed when the volume of the samples changed during dialysis, but this does not take into account PAMAM adsorption to the membrane. PAMAM-peptide conjugate solutions were also dialyzed, in order to remove any pyridine-2-thione released from the reaction between SPDP and peptides. Also here it is assumed that all PAMAM-peptide complexes stay in the dialysis tube, which is likely due to their size. If there are any peptides free in solution, they are probably also retained in the tube since their molecular weights are above 2 kDa.

In the following experiments, that investigate the interactions between DNA and PAMAM-peptide conjugates, the conjugates from Batch 3 were used.

5.2 Characterization of PAMAM-peptide conjugates

5.2.1 Mass spectrometry

Mass spectrometry was used in an attempt to characterize the PAMAM-peptide conjugates. Three samples, containing PAMAM, SN8-24 peptide and PAMAM-SN8-24 (from Batch 2), were analyzed. Figure 5.4 shows the chromatographic separation for the samples and blank (LC-MS grade water), where the intensity is given as a function of retention time. An average mass spectrum was extracted from each separation peak, making it possible to estimate which molecules are present in the respective peak. The blank measurement was used to exclude the peaks present in both samples and blank. The peaks from the chromatographic separation and those in the corresponding mass spectra, used in the attempt to identify the molecules, are listed in Table 5.2. The full retention time is not shown in Figure 5.4 since most of the peaks exclusive for the sample measurements were observed before time 3.5 for all samples. The raw data, including full retention time, may be found in the Appendix A.1.

Table 5.2: Chromatographic separation peak values at given retention time shown with the m/z peak value from the corresponding extracted mass spectra. The charge states and the identified molecules are shown for each m/z peak. "-" indicates that there were no identifying peaks in the mass spectrum observed at the given separation peak.

Sample	Separation peaks (time)	Identified peaks in mass spectrum (m/z)	Charge state (z)
PAMAM	0.28	652.0698	5 (PAMAM)
(M_w = 3256.18Da)		814.8360	4 (PAMAM)
		1086.1039	3 (PAMAM)
		1628.6429	2 (PAMAM)
	0.35	-	-
SN8-24	0.35	-	-
(M_w = 2329Da)	1.85	1163.8458	2 (SN8-24)
PAMAM-SN8-24	0.35-0.39	-	-
($M_w$unknown)	1.84	1163.8458	2 (SN8-24)
	3.46	-	-

For the PAMAM solution, the main intensity peaks were observed at retention times 0.28 and 0.35, see Figure 5.4. The average mass spectra extracted from them can be seen in Figure 5.5, where the intensity is given as a function of m/z. As described in Section 3.4, the charge state of the molecule may be determined by the spacing between peaks in the isotopic cluster. The highest peaks in the mass spectrum for retention time 0.28 were 652.0698, 814.8360, 1086.1039 and 1628.6429 (Figure 5.5, top). The spacing between the peaks in their respective isotopic clusters were 0.2, 0.25, 0.33 and 0.5, giving the charge states of 5, 4, 3 and 2, respectively. From Equation 3.8, the peaks and their charge states identified the molecular weight of the PAMAM dendrimer (M_w = 3256.18 Da). For retention time 0.35 (Figure 5.5, bottom), there is a wide distribution of peaks in the mass spectrum. Since the presence of PAMAM was identified from the 0.28 peak, these were not investigated further. However, it should be mentioned that the mass spectrum extracted from the 0.35 peak overlaps with some of the peaks in the spectrum extracted from the 0.28 peak. This is not surprising, since the 0.28 and 0.35 peaks are close to each other, and the signals coming from the ionized PAMAM may be seen in both. Uclés et al. [50] also investigated PAMAM G2 dendrimers using LC-ESI-qTOF-MS. They observed the same m/z peaks as in this study, which gives confidence to these results.

For the SN8-24 peptide, peaks were observed at retention times 0.35 and 1.85, and the corresponding mass spectra are plotted in Figure 5.6. The molecular weight of SN8-24 is expected to be approximately 2329 Da, based on its amino acid composition. The largest peak at retention time 1.85 (Figure 5.6, bottom) was found at 1163.8458, and it has a neighbouring peak at a distance of 0.5. This implies a charge state of 2, and from Equation 3.8 the calculated mass becomes 2326 Da. This corresponds well with the expected mass, and the peak is probably arising from SN8-24. The mass spectrum of retention time 0.35 was not investigated further, since the peptide could be identified from the 1.85 peak.

The mass spectra of the solution containing both PAMAM and SN8-24 may be seen in Figure 5.7. The peak observed at retention time 0.35 was present in all three samples and was therefore not used to assess the presence of PAMAM-peptide conjugates. The peak probably arises from impurities present in all samples. The peaks observed in the bottom panel in Figure 5.7, extracted from the peak at retention time 3.46, probably arise from small molecules, since the ions are singly charged (z=1). Thus, their m/z values

correspond to their molecular mass. The molecular weight of Sulfo-LC-SPDP, referred to as SPDP in this study, is 527.57 Da [54], and do not match any of the observed peaks in the spectrum. This indicates that free, non-conjugated SPDP was removed during the dialysis procedures and is not present in the PAMAM-SN8-24 sample.

From the mass spectrum corresponding to peak 1.84 (Figure 5.7, middle), it may be seen that the peak at 1163.8458, identified as SN8-24 before, is present. This suggests that there are free peptides in solution. The results from the conjugation of PAMAM-SPDP and the SN8-24 peptide, see Section 5.1.2, indeed indicate that not all crosslinkers were occupied by a peptide. Interestingly, the peaks used to identify PAMAM in Figure 5.5 are not present in these spectra. This indicates that there are none or few PAMAM free in solution, which clearly suggests that the conjugation was successful. Thus, they might have conjugated with one or more peptide, or aggregated with each other.

The main goal of these experiments was to identify and characterize the possible conjugates in solution. This turned out to be challenging for several reasons. Firstly, there were no peaks that could easily be assigned to a particular mass in the mass spectra of the PAMAM-SN8-24 solution. However, this does not mean that there are no conjugates present. Firstly, destabilizing effects, such as charge repulsion, often affect the formed ionic complexes, and the required transfer into gas phase in the mass spectrometer is not always straightforward. Also, the detection of larger molecules with high m/z ratios is generally more difficult compared to smaller molecules with low m/z ratios [59]. Secondly, even with clear peaks to assign, their interpretation of would have been challenging, since the masses of the conjugates are hard to predict in advance. It is possible to obtain the average number of peptides conjugated to PAMAM in the DTT assays, but it is unknown how the peptides are distributed among the dendrimers. In addition, there are SPDP attached to PAMAM which contribute to the mass of the molecules, making the number of possible combinations even larger. The expected masses are therefore difficult to predict, and the potential peaks could possibly have matched several different conjugate compositions.

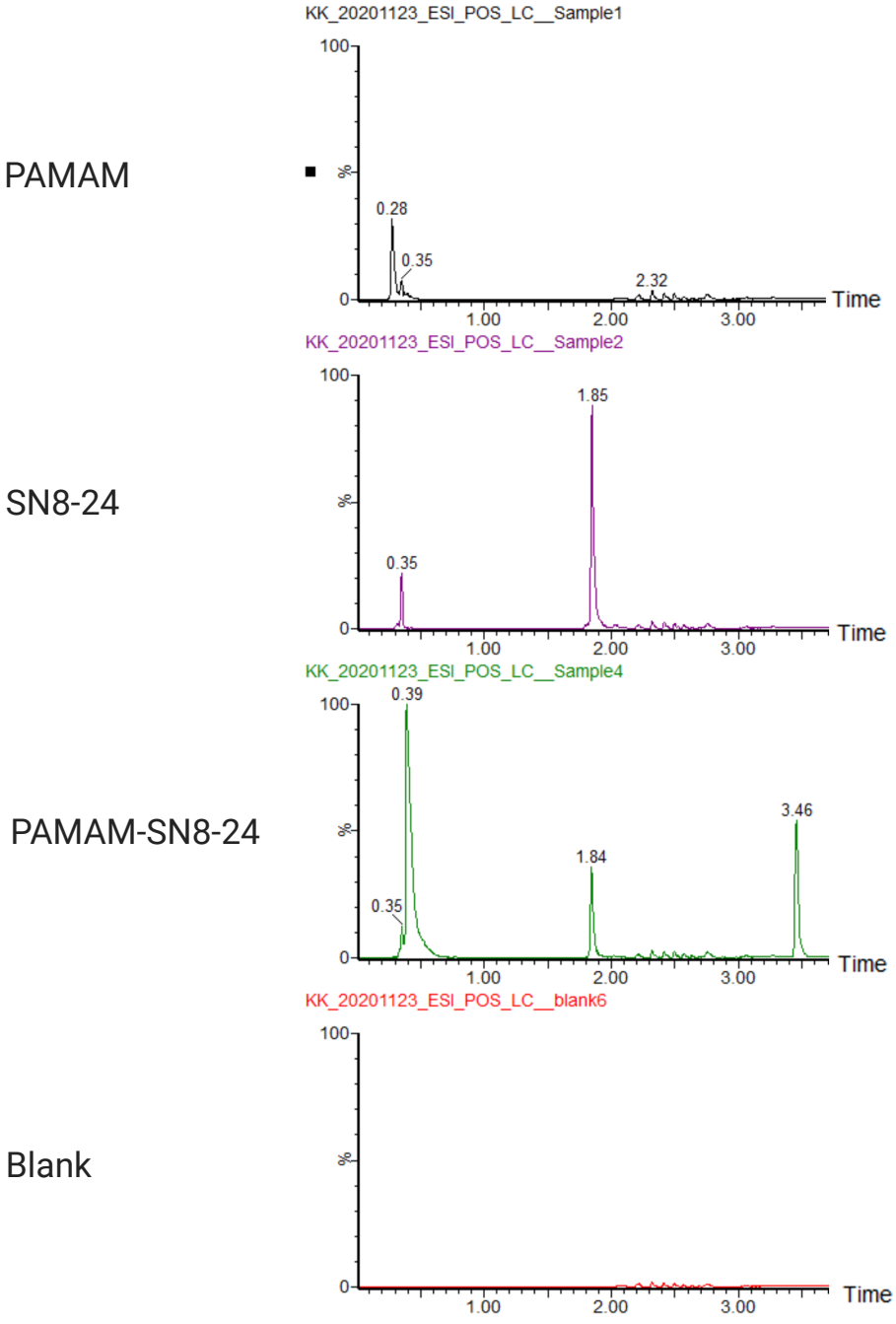

Figure 5.4: Intensity as a function of retention time for the chromatographic separation of solutions in mass spectrometry.

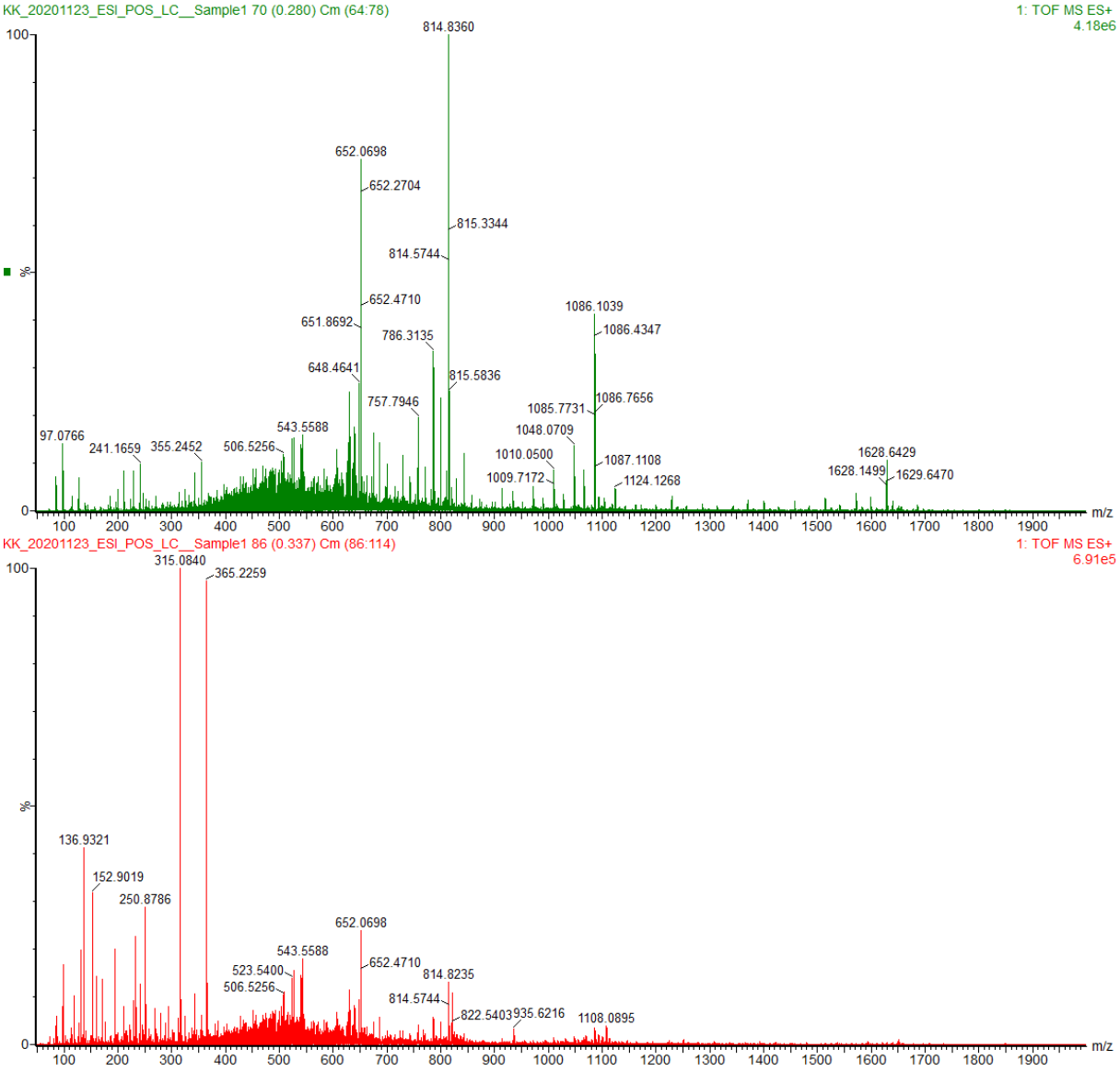

Figure 5.5: Mass spectra of the solution containing PAMAM. The spectra are extracted from the retention time peaks of 0.28 (top) and 0.35 (bottom), seen in Figure 5.5.

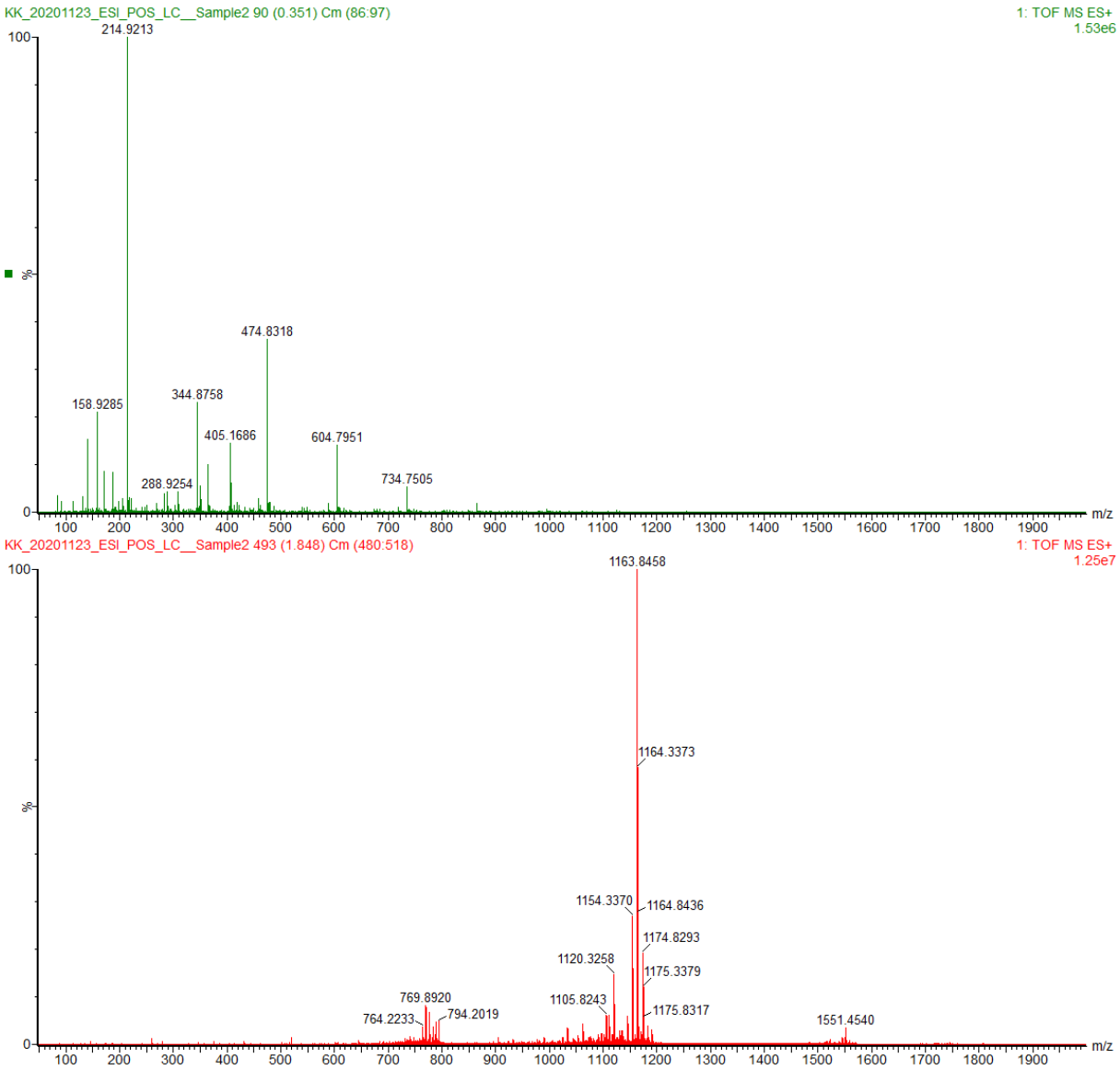

Figure 5.6: Mass spectra of the solution containing SN8-24 peptide. The spectra are extracted from the retention time peaks of 0.35 (top) and 1.85 (bottom), seen in Figure 5.5.

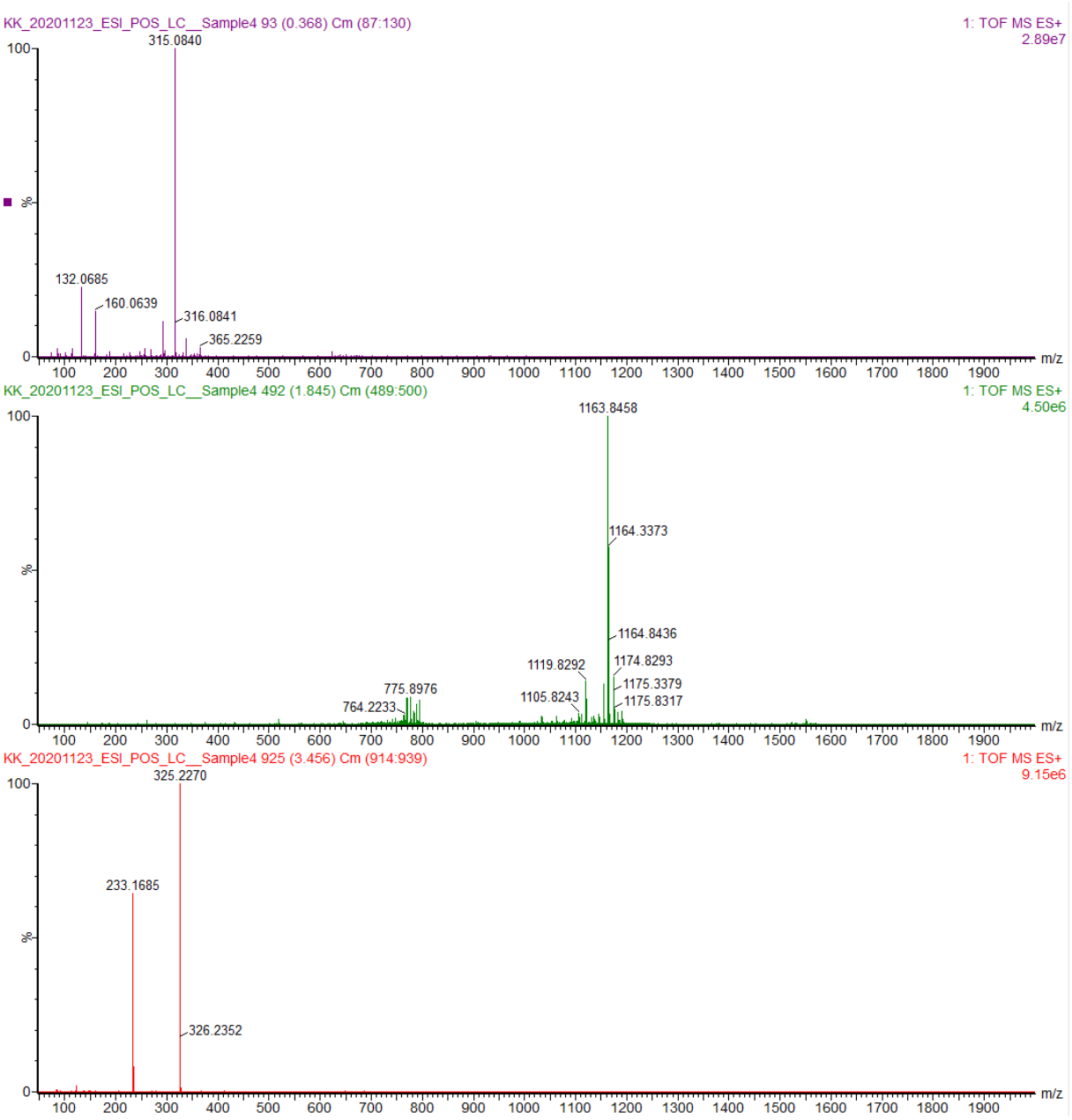

Figure 5.7: Mass spectra of the solution containing PAMAM and SN8-24 peptide. The spectra are extracted from the retention time peaks of 0.35-0.39 (top) and 1.84 (middle) and 3.46 (bottom), seen in Figure 5.5.

5.2.2 Gel electrophoresis with PageBlue Protein Staining Dye

Gel electrophoresis with PageBlue stain was also used in an attempt to characterize the PAMAM-peptide conjugates.

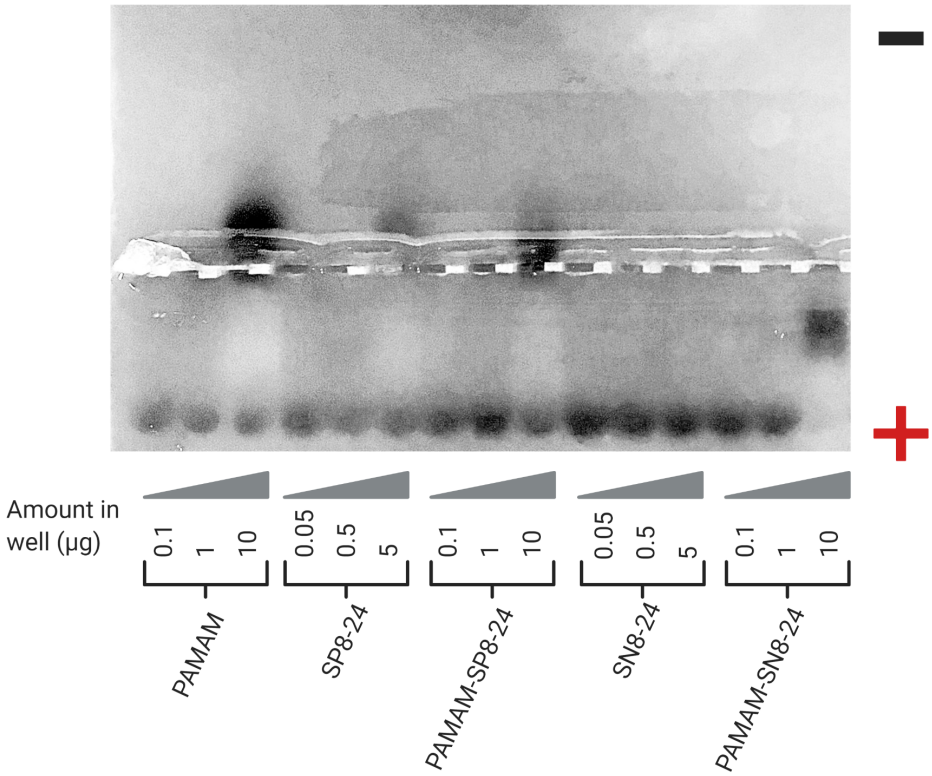

Figure 5.8: Agarose gel stained with PageBlue dye for visualization of PAMAM, peptides and PAMAM-peptide conjugates. The positions of the positive and negative electrodes are indicated with "+" and "-". The amount of molecules added to each well is shown for each sample (μg).

Figure 5.8 shows the agarose gel stained with PageBlue with PAMAM, SP8-24 peptide, PAMAM-SP8-24 conjugate, SN8-24 peptide and PAMAM-SN8-24 conjugate. This experiment was performed to investigate the possibility of detecting PAMAM and conjugates under the given conditions. For the highest amounts used ($\sim$ 10 μg), some differences between samples may be observed. The PAMAM has clearly moved towards the negative electrode, and the same goes for the PAMAM-SP8-24 conjugate. The positively charged SP8-24 peptide also shows a slight smear towards the negative electrode. This peptide is composed of serine, glycine and lysine. Lysine contains a primary amine in the end of its side group [60], which may explain why it is also visualized by the stain. For the PAMAM-SP8-24 conjugate, the dye may therefore bind to both the amine groups on the

PAMAM and the SP8-24 peptide. The negatively charged SN8-24 peptide is composed of serine, glycine and aspartic acid, which do not have any amine groups present in their side chains. This might explain why the peptide is not visible in the gel.

The band of PAMAM-SN8-24 is quite interesting, since the conjugates have clearly moved towards the positive electrode. This may imply that the negatively charged SN8-24 peptide has bound to PAMAM, making the net charge of the molecule negative. However, it seems like the PAMAM-SN8-24 also binds the loading dye, since the dye is not visible at the bottom of the lane (outermost right), as it is for the other samples.

5.2.3 Summary of characterization methods and future work

The results from mass spectrometry indicate that the PAMAM has indeed conjugated to other molecules, but exactly what type of molecules were formed is not clear. Other experimental modes of mass spectrometry should be attempted, particularly those that are better at identifying the large conjugates.

Gel electrophoresis with PageBlue staining dye was able to detect the presence of PAMAM and PAMAM-peptide conjugates, and it should be useful to try the other conjugates. However, the average number of conjugated peptides and the structure of the obtained molecules are still unknown. Some adjustments in the procedure can be made to improve visualization. The protocol states that the dynamic range of the stain is 5-500 ng, but in the present experiment, the molecules were not visualized for lower amounts than 5-10 μg. Sharma et al. [57] used mini gels, which are smaller and thinner than the gel made here. The protocol of PageBlue also indicate the use of mini gels. A thinner gel might make the staining more efficient, and less staining solution will be needed to cover the gel. The results suggest that the loading dye interferes with the samples, so this should not be used in future experiments.

Dynamic light scattering (DLS) was also attempted in this study, to investigate the size/hydrodynamic radius of the molecules. However, the results were not included, since the analyzing program reported that the samples were too polydisperse to analyze and/or the data quality was poor. This should be attempted again using more careful procedures for sample preparation, such as the filtering of the buffer solution prior to the measurements. In addition, the ideal measuring conditions for these measurements, in terms of

conjugate concentration, need to be assessed.

The main goal of this study was to investigate the impact of varying peptide composition on the binding between DNA and peptide-conjugated PAMAM molecules. Using a simplified model, the peptides mimic the disordered regions in DNA-binding proteins, while PAMAM resembles the DNA-binding domains.

Since the used peptides possess the potential to covalently bind to the PAMAM dendrimers with both ends, the resulting complexes could be PAMAM with a number of peptide tails, likely between 1 and 3, taking into account the measured average number of 2.34. It is also possible that one peptide bridges two PAMAM dendrimers forming a linker between them. However, considering that the concentration of PAMAM in the samples was not that high (0.1 mM), and the fact that they are highly charged, suggests that the likelihood of forming dimers is not high. The results from mass spectrometry and the DTT assay, see Section 5.1.2, imply conjugation of PAMAM and peptides, but the structures of the resulting molecules are not possible to determine.

The calculations made in the following experiments involving PAMAM-peptide conjugates are based on the assumption that a PAMAM-peptide conjugate is one dendrimer with connected disordered tails, rather than two or more PAMAM connected by flexible linkers. Although the assumption might be incorrect, it makes it possible to compare the different PAMAM-peptide conjugates in the interactions with DNA. The calculations based on this assumption will be discussed below.

5.3 Dye exclusion assays

5.3.1 Relationship between DNA concentration and fluorescence intensity

Fluorescence emission of GelStar bound to DNA as a function of increasing DNA concentrations is shown in Figure 5.9. The intensity is measured at 535 nm and normalized to the value measured at maximum DNA concentration of 4.9 μg/mL. The GelStar dye concentration is x10 in all samples. Linear regression was performed, resulting in the line $y = 0.20x - 0.02$, and the relationship between fluorescence intensity and DNA concentration is clearly linear. All DNA added to the solution is in “free", non-compacted form and available to the GelStar dye. Thus, the results are not surprising.

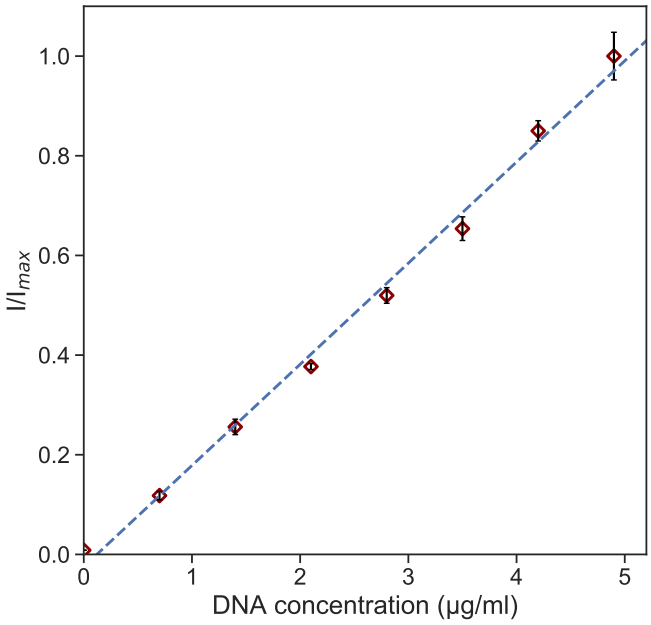

Figure 5.9: Fluorescence emission of GelStar bound to DNA as a function of increasing DNA concentrations. Linear regression was performed, resulting in the relationship $y = 0.20x - 0.02$.

5.3.2 Optimization of dye exclusion assay

Different protocols were tried for the optimization of the dye exclusion assays. The results are shown in Figure 5.10a, where each protocol was performed with constant salmon sperm DNA concentration and increasing PAMAM concentration. The intensities of the samples are measured at 535 nm and normalized to the intensity corresponding to DNA and GelStar only, $I_{\max}$. These are presented as a function of the r_{charge}, that is, the electrostatic ratio between the positive charges on PAMAM dendrimers and the negative charges on the DNA. The samples were made in triplicates, and the results are shown as means with standard deviations.

Protocol 1 was performed twice (blue and green symbols), where GelStar, DNA and buffer was mixed and equilibrated for 15 minutes before adding PAMAM. The results were inconsistent and showed large error bars. Therefore, Protocol 2 was attempted (red circles), where PAMAM, DNA and buffer were mixed and equilibrated for 15 minutes before adding GelStar. Here, the error bars were smaller. The intensity was also found to decrease faster at lower r_{charge} when compared to the first protocol. Protocol 3 is similar to protocol 2. However, in protocol 3 (yellow squares), equal volumes of DNA and PAMAM were mixed for 2 hours before adding GelStar, without the additional step of adding buffer. As expected, the results from these two protocols were quite similar. It may be that the samples do not need 2 hours to equilibrate, and the additional time might be unnecessary. However, since the transition from free to condensed looks smoother, protocol 3 was chosen for the following experiments where the interactions between DNA and different PAMAM-peptide conjugates were investigated. In addition, the mixing of equal volumes DNA and PAMAM was more effective.

The type of DNA was changed from salmon sperm to Oct-1 during the experimental process, due to the visualization of bands in gel electrophoresis. Another dye exclusion assay was therefore performed in order to compare the condensation by PAMAM dendrimers on the different DNA types. This may be seen in Figure 5.10b. The results are quite similar between the salmon sperm (yellow squares) and the Oct-1 (purple diamonds), but the Oct-1 drops more steeply with increasing r_{charge} than the salmon sperm. However, this is not deemed important in this case, since Oct-1 was used in all following experiments. An assay with Oct-1 DNA, using ethidium bromide (EtBr) as dye, is also

shown in Figure 5.10b (brown circles). The intensities were measured at 600 nm and normalized to the intensity corresponding to DNA and EtBr only, I_{max}. Surprisingly, there was only a small decrease in intensity with increasing r_{charge} compared to the assays performed with GelStar. In addition, the normalized intensity of the control sample with EtBr and buffer was 0.56. This intensity is expected to be approximately 0, due to the absence of DNA, and the reason for the high value is unclear. However, this was not investigated further, since the assays performed with GelStar gave satisfying results, and GelStar was used in all following experiments.

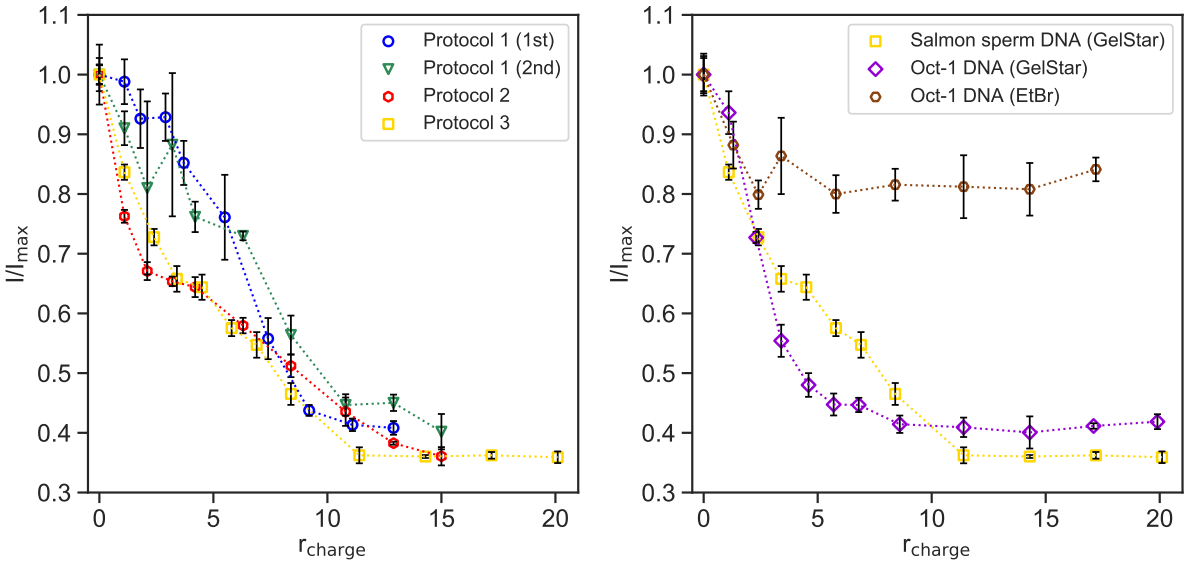

Figure 5.10: Normalized fluorescence intensity from DNA-GelStar (at 535 nm) or DNA-EtBr (at 600 nm) complexes as a function of increasing r_{charge} between positive charges on PAMAM dendrimers and negatively charged phosphate groups in DNA. Figure (a) shows the comparison of different protocols used for constant salmon sperm DNA and increasing PAMAM dendrimer concentrations with GelStar as dye. Figure (b) shows the comparison of constant salmon sperm and Oct-1 DNA with increasing PAMAM dendrimer concentrations, where protocol 3 and GelStar were used in both cases. In addition, an assay using Oct-1 DNA and EtBr as dye is shown in the same figure.

5.3.3 Dye exclusion with PAMAM-peptide conjugates

Figures 5.11 and 5.12 show the dye exclusion assays performed with conjugated PAMAM-peptide complexes, but using different variables on the x-axes, that is with the normalized fluorescence intensity as a function of r_{molar} and r_{charge}, respectively.

r_{molar} is defined as the ratio between the number of PAMAM or PAMAM-peptide conjugates added per Oct-1 DNA molecule in solution. The average number of SPDP crosslinkers attached to the dendrimers was calculated to be 2.34, see Table 5.1, and the peptides were added with a peptide:SPDP of 1. Consequently, the expected average number of peptides per PAMAM is 2.34, based on the assumption that all peptides added to the solution are conjugated to PAMAM dendrimers. One molecule is therefore approximated to be a PAMAM molecule with an average of 2.34 peptides attached. Considering that the absorption of pyridine-2-thione before and after addition of DTT, see figure 5.3, was almost the same for most samples, this assumption is deemed reasonable. However, it may be seen that the assumption might not be valid for all PAMAM-peptide solutions. For example, for the solutions where peptides S-25 and SP-25 are added, the absorbance after the addition of DTT is much higher than before the addition, which indicates that some SPDP on the dendrimers are non-occupied, and that some peptides are free in solution. It is also assumed that each peptide has attached to one dendrimer only, based on the low concentration and high charge of PAMAM (0.1 mM), as discussed in Section 5.2.3. The number of DNA molecules is calculated from the known concentration and size of Oct-1 (3605 bp) in solution.

r_{charge} is calculated from the net charge of the PAMAM or PAMAM-peptide conjugates divided by the total number of negatively charged phosphate groups in the DNA. As before, it is assumed that all peptides added have attached to one dendrimer. Each dendrimer is expected to have 16 positively charged amine groups on their surface under the given conditions. However, when the SPDP crosslinker binds, it neutralizes the charge of the amine group. Therefore, given that in average 2.34 crosslinkers have attached per dendrimer, 2.34 positive charges are subtracted from each dendrimer in the calculation of r_{charge}. The peptides were added with a peptide:SPDP of 1. The net charge of the PAMAM-peptide conjugates therefore becomes the corrected dendrimer charge, in addition to the total charge of the added peptides. The number of negatively charged phosphate groups is calculated from the known DNA concentration. Two different PAMAM-peptide concentration ranges were used when studying these complexes, depending on the charge of the peptide conjugated. For the conjugates with positively charged peptides, the intensity was expected to drop at lower ratios than for the ones

with negatively charged or neutral peptides. Thus, the curve will flatten at a lower ratio and a smaller concentration range was used for the conjugates with positively charged peptides.

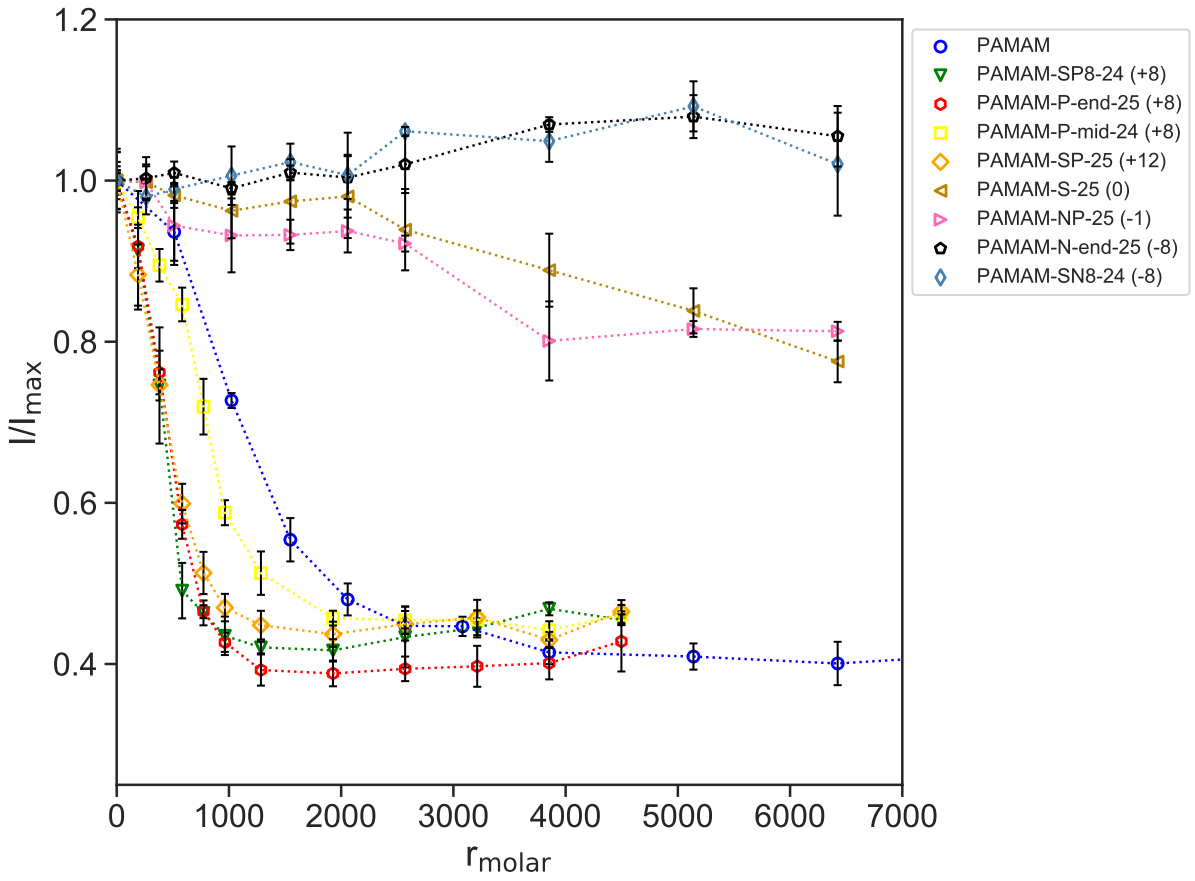

Figure 5.11: Normalized fluorescence intensity as a function of r_{molar}. The ratio is defined as number of PAMAM-peptide conjugates added per Oct-1 DNA molecule. The assay was performed for PAMAM alone and all PAMAM-peptide conjugates, and the charge of the respective peptide is shown in parenthesis. For the PAMAM alone, the ratio is defined as PAMAM molecules per DNA molecule.

From Figure 5.11, some trends are visible. For the PAMAM-peptide conjugates with positively charged peptides (+8 or +12), the fluorescence intensities decrease at lower molar ratios than for PAMAM alone. This is as expected, since the conjugates have a higher net positive charge per molecule. They are therefore more efficient in inducing DNA condensation, and consequently reduce the fluorescence intensity of GelStar. One might have also expected that the PAMAM-SP-25 (+12) would show a steeper decrease than the other conjugates with peptide charge of +8, but this is not seen. PAMAM-P-mid-24

differs from the other conjugates containing positively charged peptides, by requiring a larger number of dendrimer conjugates to decrease fluorescence.

For PAMAM-S-25 (0) and PAMAM-NP-25 (-1), the intensity decreases for much higher ratios than for PAMAM and the conjugates discussed above, and the decline is remarkably less steep. This suggests that the conjugated peptides hinder to some extent the binding of PAMAM to DNA, and preventing its condensation. It is also possible that the dendrimers bind to DNA but the neutral peptides prevent condensation.

For PAMAM-N-end-25 (-8) and PAMAM-SN8-24 (-8), the intensity is nearly constant, or slightly increases, for all studied ratios. The negatively charged peptides conjugated to PAMAM seem to completely prevent the binding of the conjugates to DNA. It is likely that the peptides adsorb strongly to the PAMAM surface charged groups, and since it is assumed that in average 2.34 peptides are bound to each PAMAM, the overall charge of the complexes becomes negative. Consequently, the complexes may not bind to DNA due to electrostatic repulsion.

A dye exclusion assay was also performed for the PAMAM-SN8-24 conjugates, prepared from Batch 2, with salmon sperm DNA. The results may be found in Appendix A.2. Surprisingly, these results showed a large intensity increase for increasing r_{molar}. Control samples were made with SN8-24 and DNA with GelStar, and PAMAM-SN8-24 with GelStar. These indicated that neither SN8-24 or PAMAM-SN8-24 were able to bind GelStar and thereby increase the fluorescence intensity. The reason for the large increase in intensity, when DNA was mixed with the PAMAM-SN8-24 conjugates, is therefore not clear. Also, when the assay was performed for PAMAM-SN8-24 in Experiment 3, the intensity remained constant for increasing r_{molar}. The reason for the difference between experiments is also unclear.

The results in Figure 5.11 are also displayed as fluorescence intensity as a function of r_{charge} in Figure 5.12. The conjugates with peptide charges of -8 were excluded, since the calculated overall charge of them becomes negative and gives a r_{charge} of opposite sign. As observed in Figure 5.11, PAMAM-SP8-24 (+8) and PAMAM-P-end-25 (+8) seem to compact DNA more efficiently with the fluorescence intensity decreasing more strongly at low r_{charge}. However, PAMAM-SP-25 (+12) and PAMAM show a more similar behaviour when compared to the plot in function of r_{molar}. Regarding P-mid-24 (+8), the decrease

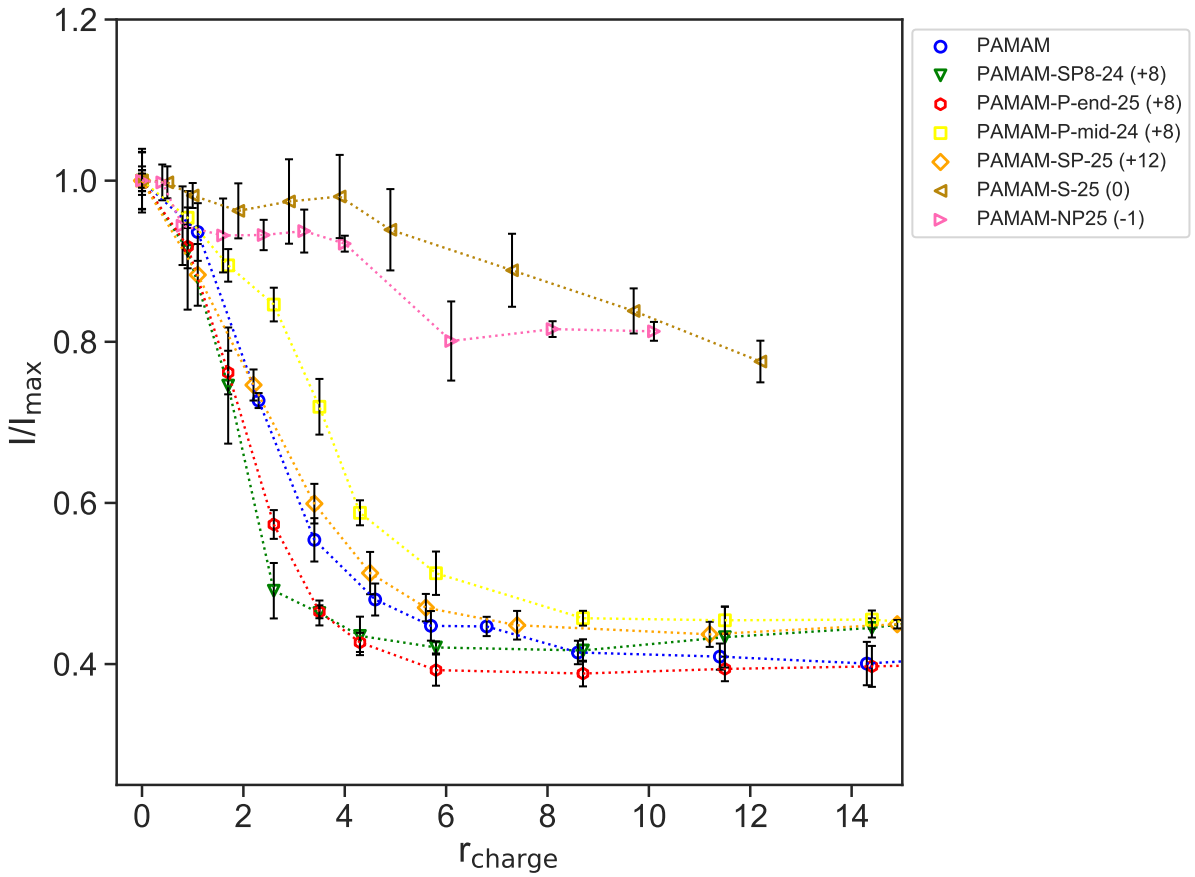

Figure 5.12: Normalized fluorescence intensity as a function of r_{charge}. The ratio is defined as the total number of charges on the PAMAM-peptide conjugates divided by the total number of negatively charged phosphate groups in the DNA. The assay was performed for all PAMAM-peptide conjugates, and the charge of the respective peptide is shown in parenthesis.

in fluorescence occurs at a higher r_{charge} than PAMAM alone, which is also in contrast to results from Figure 5.11. PAMAM-S-25 (0) and PAMAM-NP-25 (-1) show the same trends as before.

The two ways of presenting the results, using r_{molar} and r_{charge}, may both be informative. For r_{molar}, it is clear that the conjugates with positively charged peptides are more efficient in condensing DNA compared to the same number of PAMAM molecules without peptides. However, assuming that indeed an average of 2.34 peptides are attached per PAMAM, the charge per molecule is approximately doubled for the conjugates with peptides of charge +8 compared to a PAMAM molecule alone. It is therefore not surprising that they are better at condensing the DNA than PAMAM. Therefore, it may also be interesting to look at the r_{charge}, where the ratio is based on the number of charges

present. Here, the differences are less clear between PAMAM alone and the conjugates with positively charged peptides. The PAMAM-SP8-24 (+8) and PAMAM-P-end-25 (+8) have the steepest curves in both figures, suggesting that they are more efficient in DNA condensation. However, the differences from curves corresponding to PAMAM and the other conjugates with positively charged peptides are not that large.

Three control samples were made in each experiment, including PAMAM-peptide conjugates without DNA, and peptides alone with and without DNA. All samples contained the same amount of GelStar as above. For all PAMAM-peptide conjugates and peptides, the fluorescence intensity was approximately zero in the absence of DNA. Thus, the molecules themselves do not bind GelStar.

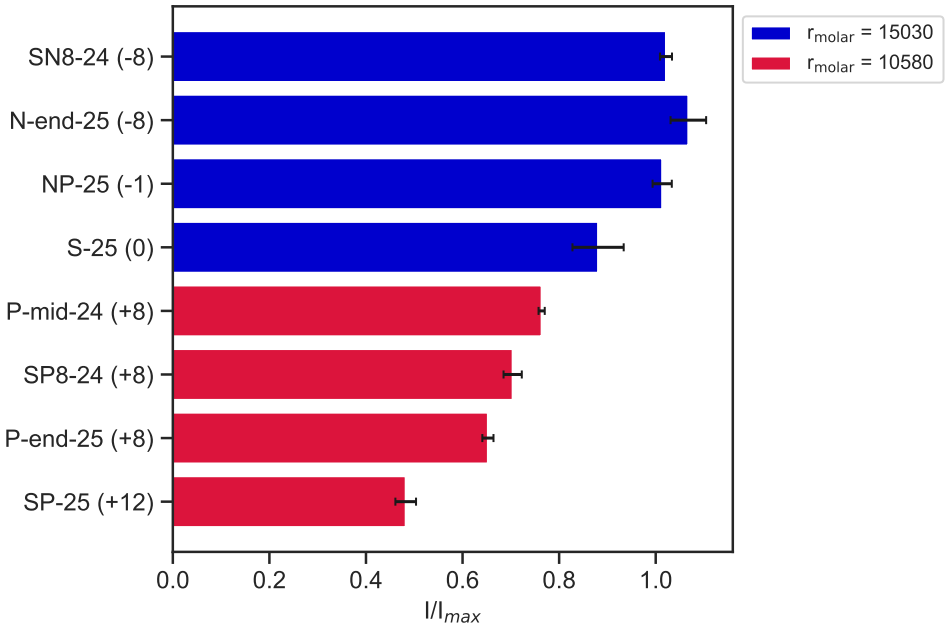

Figure 5.13: Normalized fluorescence intensity shown for peptides at a given r_{molar}, with the same DNA concentration. The peptide-DNA solutions served as control samples in their respective dye exclusion assay performed with the PAMAM-peptide conjugates. The intensities are normalized to the I_{max} in the given experiment.

In the samples containing peptides and DNA, the results varied according to the peptides, see Figure 5.13. For the positive SP8-24 (+8), P-end-25 (+8), P-mid-24 (+8) and SP-25 (+12), the fluorescence intensity decreased when the peptides were present compared to the intensity measured for DNA alone. Only one concentration was probed, $r_{\text{molar}} = 10580$, defined as number of peptides per DNA molecule. SP-25 was the most

effective. For NP-25 (-1), N-end-25 (-8) and SN8-25 (-8), there were no decrease in fluorescence intensity. For the neutral peptide, S-25 (0), there was a small decrease in intensity. These results indicate that the positively charged peptides bind to and induce some condensation on DNA, while the negative peptides do not, as expected. Surprisingly, the neutral peptide also seems to condensate the DNA slightly. Two different concentration ranges were used in the assessment of PAMAM-peptide conjugates, one for the positively charged peptides and one for the others. The peptide concentration in the control samples corresponded to the concentration of peptides in the highest PAMAM-peptide solution. Therefore, the non-positively charged peptides were added with a different r_{molar} than the positively charged peptides, since different concentration ranges were used.

5.4 Gel electrophoresis

5.4.1 Optimizing the sample concentration range

Gel electrophoresis, with salmon sperm DNA, was performed to probe for the ratios at which condensation of DNA could be seen. $r_{\text{charge}} = r_{\text{molar}} = 0$ corresponds to samples with DNA in the absence of PAMAM.

Figure 5.14a shows the first assay performed, where the r_{charge} ranged from 0 to 20. It is clear that the DNA has left the well at ratio 0. There is also a clear decrease in the intensity of the second well at ratio 2, compared to the samples with higher ratio. The condensation of DNA seems to occur between ratios 2 and 4, therefore, a new experiment was performed with r_{charge} ranging from 0 to 5, as seen in Figure 5.14b. The intensity of the bands decrease significantly from r_{charge} 0.5 to 1.0, and most of the DNA remain in the wells for higher ratios, suggesting that the DNA is condensed.

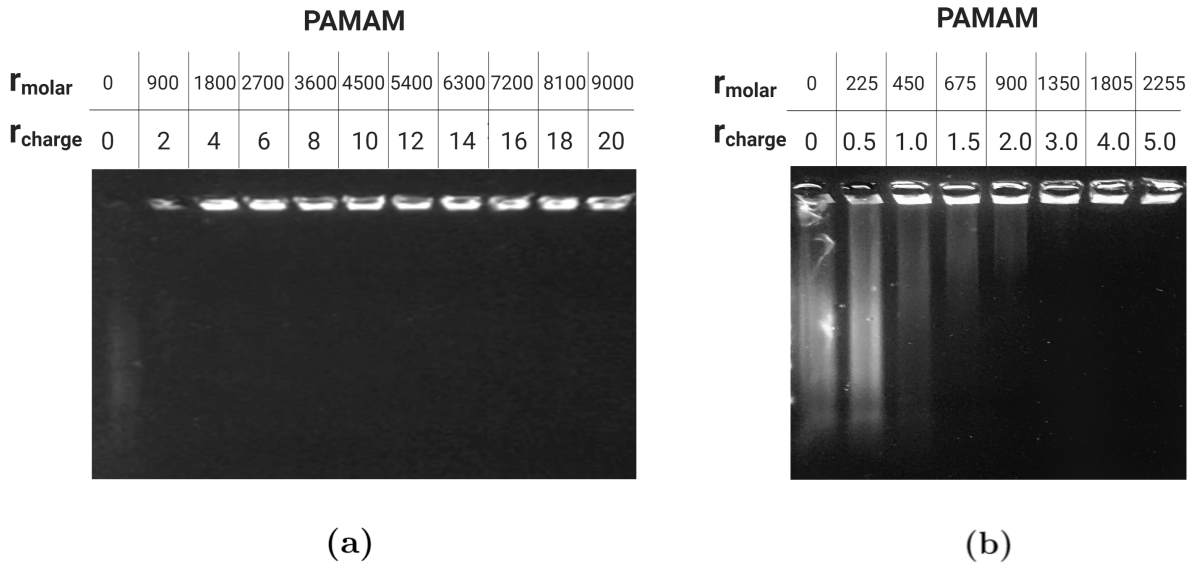

Figure 5.14: Gel electrophoresis of 25 μg/mL salmon sperm DNA with increasing PAMAM concentration. The r_{molar} represents PAMAM molecules added per DNA molecule, while the r_{charge} refers to the ratio between positively charged PAMAM surface groups and negatively charged DNA phosphate groups. The figures show assays performed with a r_{charge} ranging from (a) 0 to 20 and (b) 0 to 5.

In Figure 5.15, the same assay was performed, but with Oct-1 DNA and a r_{charge} ranging from 0 to 2. The DNA concentration was also decreased from 25 to 10 μg/mL. The Oct-1 DNA used was a plasmid, thus the bands showing relaxed, unwinded DNA molecules are also present. There is a coexistence of free and complexed/condensated DNA for $r_{\text{charge}} \leqslant 0.9$. For higher ratios, the DNA shows low electrophoretic mobility and stays in the wells. The ratios at which the DNA condensates seem to be quite similar for the salmon sperm and the Oct-1 DNA.

These results agree well with the study performed by Ainalem et al. [58]. They also saw a coexistence of free and complexed DNA for $r_{\text{charge}} \leqslant 1$. However, they used a dendrimer of generation 4, while generation 2 was used in this study. Although, it is still interesting that the charge ratio, at which all DNA is retained in the well, is approximately the same for these two different dendrimer generations.

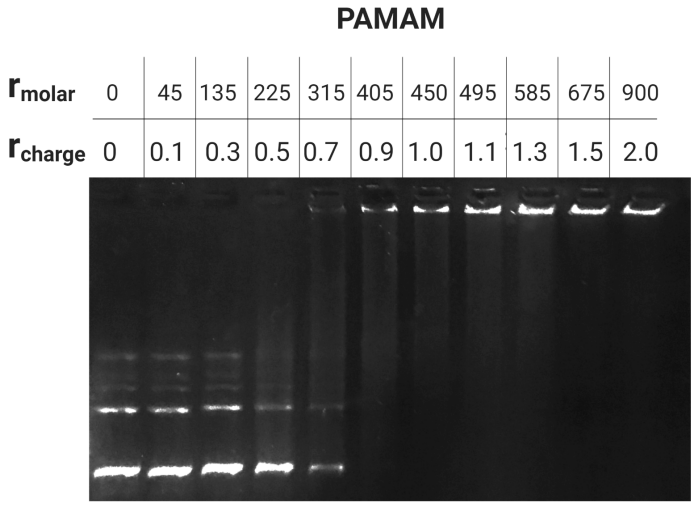

Figure 5.15: Gel electrophoresis of 10 μg/mL Oct-1 DNA with increasing PAMAM concentration. The r_{molar} represents PAMAM molecules added per DNA molecule, while the r_{charge} refers to the ratio between positively charged PAMAM surface groups and negatively charged DNA phosphate groups. The ratio of 0 corresponds to DNA only.

5.4.2 DNA condensation by peptides and PAMAM-peptide conjugates

Gel electrophoresis studies were performed for all peptides and PAMAM-peptide conjugates. The DNA used was Oct-1 with a concentration of 10 μg/mL in all gels (except for PAMAM-SN8-24, where 25 μg/mL was used), and the results are in most cases shown for both r_{molar} and r_{charge}. The DNA concentration was reduced in order to obtain the wanted r_{charge} without having to concentrate the PAMAM-peptide conjugates.

The gels showing DNA condensation by positive peptides (left hand-side panels) and the corresponding PAMAM-peptide conjugates (right hand-side panel) can be seen in Figures 5.16 and 5.17. For the peptides possessing eight positive charges, the results are quite similar. The coexistence of free and complexed DNA is most prominently seen between r_{charge} of 1.5-1.8, 1.1-1.5 and 1.3-1.5, for peptides SP8-24 (+8), P-end-25 (+8) and P-mid-24 (+8), respectively. For peptide SP-25 (+12), the coexistence occurs between r_{charge} of 0.9-1.2. These results indicate that the peptides themselves are capable of binding to and condensating the DNA, and that the SP-25 (+12) is a more effective condensing agent than the other positively charged peptides. For the conjugates PAMAM-SP8-24, PAMAM-P-end-25 and PAMAM-P-mid-24, full condensation is reached at an r_{charge} of 1.8. The ratio is around 1.3 for the PAMAM-SP-25. It may be observed that the r_{charge}, at which all DNA is complexed and remains in the wells, is quite similar for the peptides and their corresponding conjugates, when considering charge ratios.

The results can also be compared to the condensation induced by PAMAM dendrimers without conjugated peptides, where full condensation was reached at r_{charge} of 0.9. The corresponding r_{molar} was 405 PAMAM per DNA molecule. Interestingly, the r_{molar}, at which the PAMAM-peptide conjugates with peptide charge of +8 condensate the DNA, is also found to be 405 PAMAM-peptide conjugates per DNA (corresponding to the r_{charge} of 1.8). This indicates that the presence of peptides does not affect the condensation, since the same amount of molecules is needed. This is quite surprising, since the peptides themselves were found to be able to condensate the DNA, and the dye exclusion assays indicate a larger condensation by conjugated dendrimers. On the other hand, for PAMAM-SP-25, the addition of peptides increased the condensation and only 225 molecules per DNA was

required to complex and retain all DNA in the well.

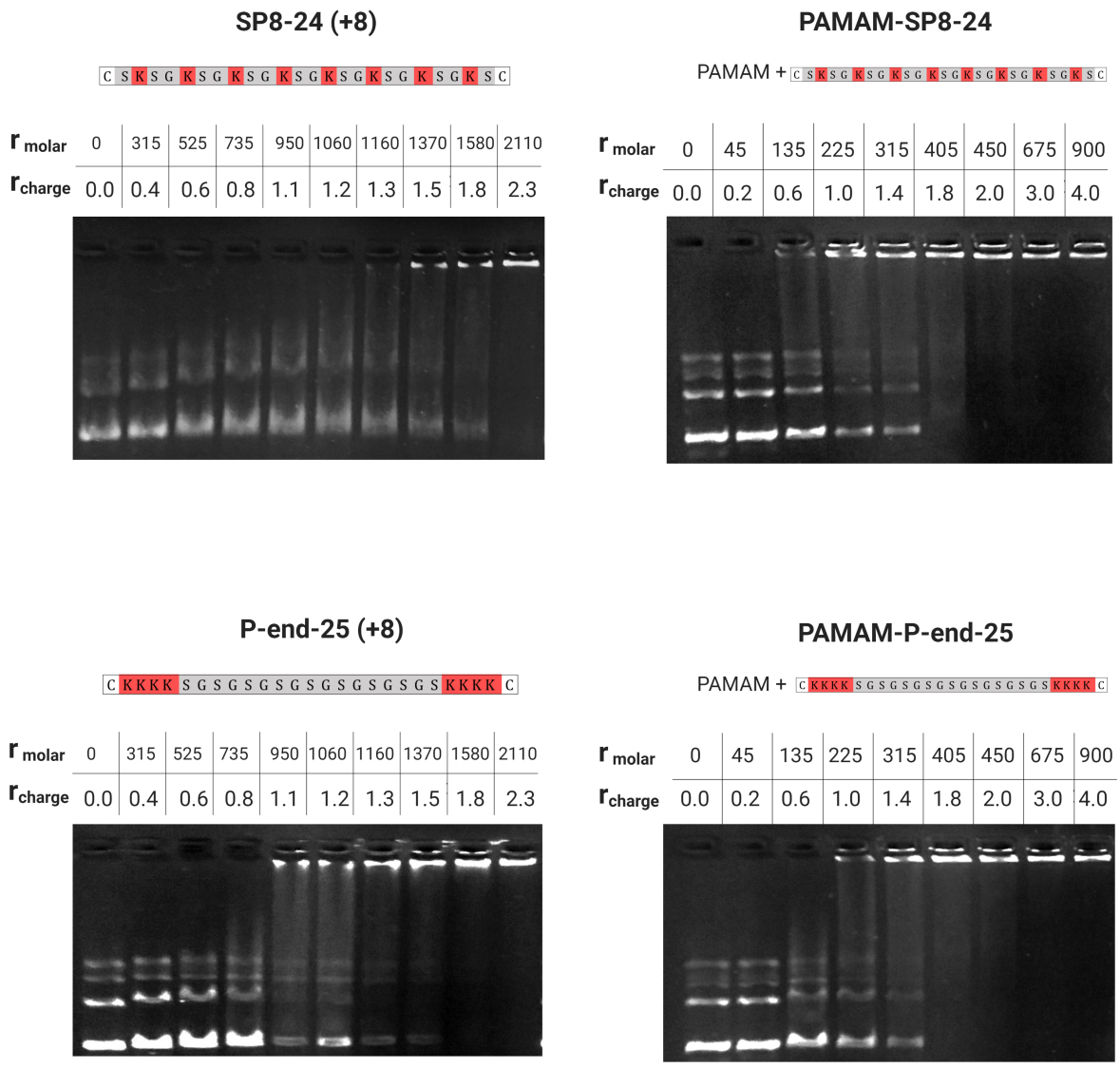

Figure 5.16: Gel electrophoresis of 10 μg/mL Oct-1 DNA with increasing concentrations of SP8-24 and P-end-25 peptides (left) and PAMAM-SP8-24 and PAMAM-P-end-25 conjugates (right). The peptide charges and compositions are shown. The r_{molar} represents PAMAM molecules added per DNA molecule, while the r_{charge} refers to the ratio between positively charged PAMAM surface groups and negatively charged DNA phosphate groups. The ratio of 0 corresponds to DNA only.

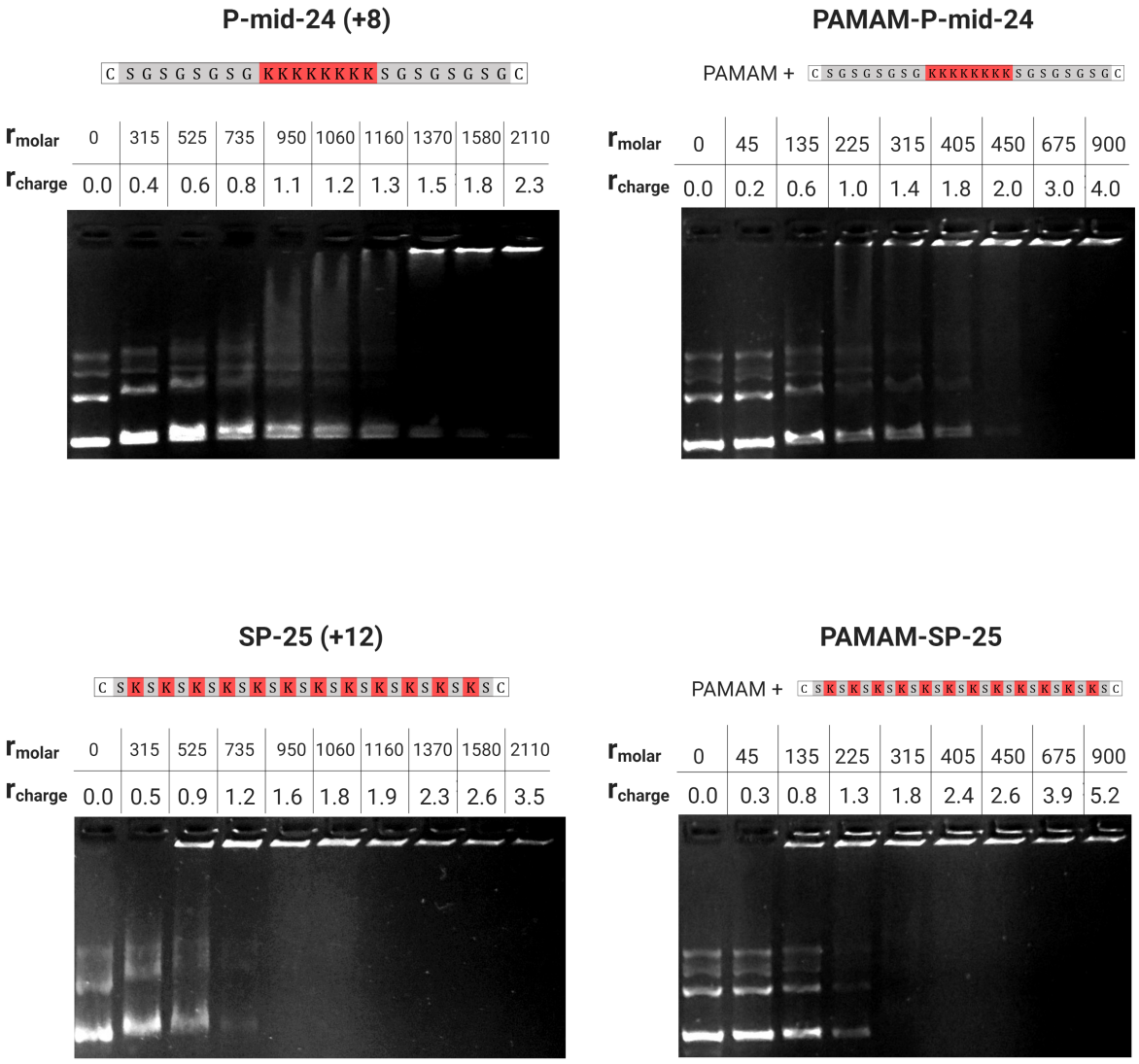

Figure 5.17: Gel electrophoresis of 10 μg/mL Oct-1 DNA with increasing concentrations of P-mid-24 and SP-25 peptides (left) and PAMAM-P-mid-24 and PAMAM-SP-25 conjugates (right). The peptide charges and compositions are shown. The r_{molar} represents PAMAM molecules added per DNA molecule, while the r_{charge} refers to the ratio between positively charged PAMAM surface groups and negatively charged DNA phosphate groups. The ratio of 0 corresponds to DNA only.

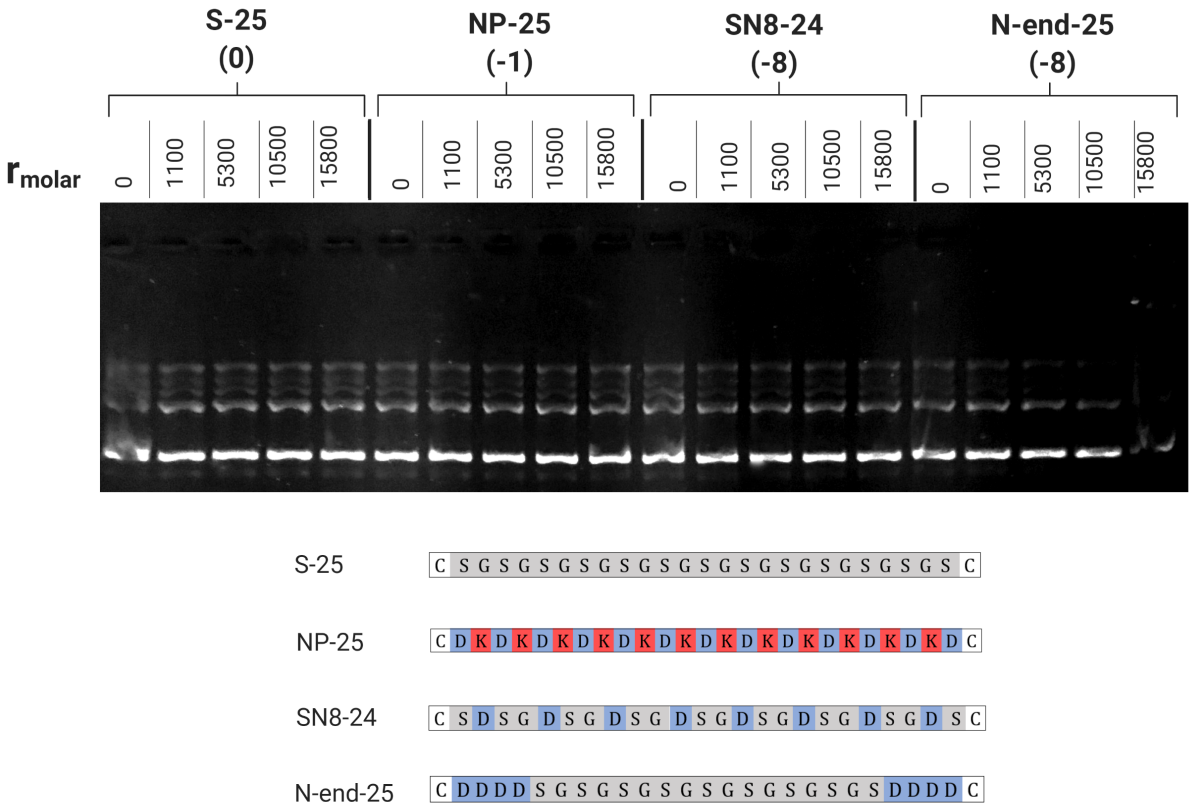

Figure 5.18: Gel electrophoresis of 10 μg/mL Oct-1 DNA with increasing concentrations of neutral and negatively charged peptides. The peptide charges and compositions are shown. The r_{molar} represents peptides added per DNA molecule. The ratio of 0 corresponds to DNA only.

Figure 5.18 shows the image of the gels obtained for samples of DNA and neutral and negative peptides. Fewer samples with larger concentrations of peptides were tested in one gel, since they were not expected to condensate the DNA, due to their charge or lack there off. Bands, referring to migrating, "naked" DNA molecules, were indeed visible for all r_{molar}. The corresponding r_{charge} is not shown, since both peptides (except S-25) and DNA are negatively charged. The outermost right and left bands are slightly unclear, but this is probably due to deformations in the gel.

Figure 5.19 shows the gels performed with PAMAM-peptide complexes with neutral or negative peptides. For PAMAM-S-25, most of the DNA is retained in the well at a r_{charge} of 6.4. However, the condensation is also evident at ratio 4.3. For PAMAM-NP-25, most of the DNA remains in the well at r_{charge} 3.5 and is completely retained at ratio 5.3. However, when looking at r_{molar}, the DNA condensation occurs at the same number of

conjugates per DNA molecule, namely 2255. Thus, the effect of one single charge in the overall neutral peptide chain does not seem to have a large impact on DNA condensation.

As for the negative peptides alone, the DNA travels through the gel at all ratios for PAMAM-SN8 (-8) and PAMAM-N-end-25 (-8). This implies that the negative peptides prevent the PAMAM from binding to the DNA.

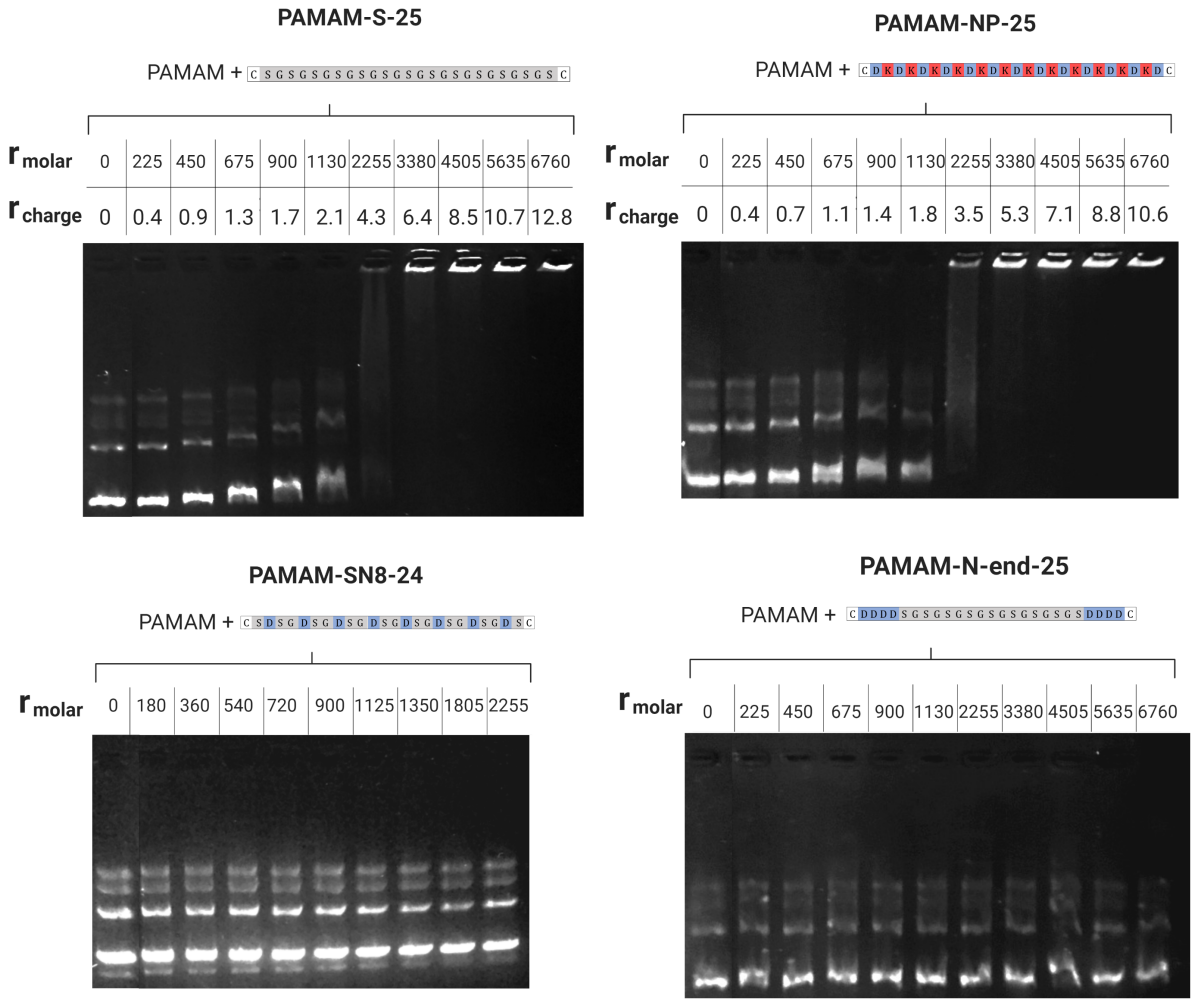

Figure 5.19: Gel electrophoresis of 10 μg/mL Oct-1 DNA with increasing concentrations of PAMAM-S-25, PAMAM-NP-25, and PAMAM-N-end-25 conjugates (25 μg/mL Oct-1 DNA was used for PAMAM-SN8-24). The corresponding peptide charges and compositions are shown. The r_{molar} represents PAMAM molecules added per DNA molecule, while the r_{charge} refers to the ratio between positively charged PAMAM surface groups and negatively charged DNA phosphate groups. The ratio of 0 corresponds to DNA only.

5.5 Summary of gel electrophoresis and dye exclusion assays

DNA condensation by PAMAM dendrimers, peptides and PAMAM-peptide conjugates was studied with both dye exclusion assays and gel electrophoresis.

The DNA concentrations used were 2 μg/mL and 10 μg/mL in dye exclusion and gel electrophoresis, respectively. The r_{charge} and r_{molar}, where the condensation of DNA is observed, are significantly higher in the dye exclusion assays compared to in the gels. This suggests that a higher number of condensing molecules, or number of positive charges, per DNA is required in order for condensation to occur at lower DNA concentrations. The ratios are therefore not directly comparable between methods, but it is possible to observe and compare trends.

For the conjugates with positively charged peptides, the results were quite consistent between methods, but differed at some points. Figure 5.12, with intensity as a function of r_{charge}, shows that the PAMAM and the conjugates have the same decreasing trend in the dye exclusion assays. There are some differences between conjugates, and the PAMAM-SP8-24 and PAMAM-P-end-25 seem to condensate the DNA at lowest ratios. They are however not very different from the other conjugates, and this may also be seen in the corresponding gels. However, for r_{molar} in the dye exclusion assays, there is a clear difference in condensation of DNA between PAMAM and the PAMAM-peptide conjugates with peptides of charge +8. The condensation induced by the conjugates is seen at lower r_{molar} than by PAMAM only. This is expected since the overall charge per molecule is higher for the conjugates. In contrast, the difference is not seen in the gels, where the r_{molar} for which the DNA remains in the wells is equal for PAMAM and the PAMAM-peptide conjugates. The reason for this in unclear, and the differences in the experimental setup do not explain the differences observed. Also, the differences between the conjugates possessing peptides of equal overall charge, but different amino acid distribution, were too small to draw any conclusions regarding the impact of amino acid architecture.

PAMAM-SP-25 (0) and PAMAM-NP-25 (-1) showed the same trends in both methods. In the dye exclusion assays, there was a moderate decrease in fluorescence intensity for increasing concentration of both conjugates. This was also seen in the gels, where the

condensation occurs, but at a much higher ratios than for the PAMAM and the conjugates with positively charged peptides. The moderate decrease suggests that the peptides prevent DNA condensation. The most likely explanation for this is that PAMAM binds to DNA, but its tails prevent, to some extent, condensation of the DNA molecule. If there are approximately two tails present on each PAMAM, and the tails are neutral or have a net charge of -1, the overall charge of the conjugate will still be positive. It is therefore likely to interact electrostatically with the DNA. On the other hand, the steric repulsion induced by the tails will prevent condensation. There is also a possibility for the tails to prevent the PAMAM-conjugate from binding to DNA altogether, but this is less likely, due to the high overall charge. It should also be noted that the amino acid composition of the two conjugated peptides are very different, although their overall charge only differs by a single charge. S-25 is composed solely of neutral amino acids, while NP-25 consists of alternating negatively and positively charged amino acids. However, they show similar results, indicating that the difference in amino acid composition does not affect the binding to a large extent, as long as the overall charge is approximately the same. The amino acid compositions of S-25 and NP-25 are however not directly comparable since their overall charge differ by one. In future experiments, neutral peptides of different compositions should be compared in order to further investigate the impact of amino acid composition and distribution.

PAMAM-SN8 (-8) and PAMAM-N-end-25 (-8) did not seem to condensate the DNA at all. The fluorescence intensity was constant or slightly increased in the dye exclusion assays, and the DNA was able to move through the gel in the electrophoresis study, for all studied concentrations of conjugates added. As mentioned, the peptides may adsorb to the PAMAM surface groups, blocking the interaction with DNA, and the overall charge of the conjugates is negative. Consequently, they are not expected to bind to DNA.

Control samples of the DNA-peptide systems were made for one ratio in the dye exclusions assays, see Figure 5.13, while a concentration range was studied in the gel for each peptide. For the negatively charged peptides, the results are consistent. It is clear that they do not condensate the DNA. For S-25, there is a small decrease in fluorescence intensity at the given ratio. This effect is not seen in the gel, where the DNA behaves as for the negatively charged peptides, see Figure 5.18. For the positively charged peptides,

the trends are also similar in the two methods. SP-25 (+12) is more effective than the other positively charged peptides of charge +8, based both on r_{charge} and r_{molar}. The peptides of charge +8 have the same overall charge, but different charge distributions. It is not possible to assess if the charge distribution affects the binding of the peptide to DNA from these results, since there is no clear difference between them.

Chapter 6

Conclusion

In this work, the impact of peptide composition on the binding between DNA and PAMAM-peptide conjugates was studied. The peptides resembled disordered regions in DNA-binding proteins, due to their extended conformation and lack of structure, while the positively charged PAMAM dendrimers mimicked DNA-binding domains.

Since the characterization of the resulting molecules turned out to be challenging, it was not possible to determine the composition of the resulting conjugated molecules in the solution during the period of this work. However, there was enough evidence to conclude that dendrimers with conjugated tails were obtained. Dye exclusion assays and gel electrophoresis studies showed that the peptide composition affects the interactions between DNA and peptide-conjugated PAMAM dendrimers. The dendrimers bind non-specifically to DNA, and the strength of the interactions was probed assuming that the most efficient condensing agents also bind the strongest. Not surprisingly, peptides of different overall charge affected the binding differently. For the PAMAM conjugated with negatively charged peptides, no DNA condensation was observed. This suggests that the conjugates were completely prevented from binding to DNA, due to an overall negative charge of the complexes. The conjugates possessing neutral and singly negatively charged peptides were able to condense DNA to some extent, but less efficiently, when compared to the PAMAM only. This suggests that the conjugates bind to DNA, but the tails hinder further condensation. In comparison to PAMAM only, the conjugates possessing positively charged peptides were found to condense DNA more efficiently or to approximately the same extent, depending on the experimental method used. The

differences between peptides of the same overall charge, but with different amino acid composition, were found to be too small to draw conclusions regarding the impact of peptide architecture on the interactions between the conjugates and DNA. Other assays or experimental techniques should be attempted to highlight the potential differences, for example, enzyme digestion assays.

Future work should also focus on the characterization of the PAMAM-peptide conjugates and improving protocols for mass spectrometry, dynamic light scattering, and gel electrophoresis. Molecular modeling may provide molecular details on the interactions of conjugates and complex formation with DNA, and should also be investigated.

This work focused on the effect of peptide composition on the strength of non-specific binding between molecules and DNA. Thus, the binding kinetics and diffusion rates of conjugates along DNA were not investigated. Diffusion measurements, including synthesized peptide-conjugated DNA-binding proteins that bind to a specific target sequence, could therefore also be attempted.

Bibliography

[1] J.A. Drake and B.M. Pettitt. Physical chemistry of the protein backbone: Enabling the mechanisms of intrinsic protein disorder. *The journal of physical chemistry. B*, 124(22):4379–4390, 2020.

[2] A.K. Dunker, C.J. Brown, J.D. Lawson, L.M. Iakoucheva, and Z. Obradović. Intrinsic disorder in cell-signaling and cancer-associated proteins. *Journal of Molecular Biology*, 323(3):573–584, 2002.

[3] J. Hardin. *Becker's world of the cell.* Pearson, 9th edition, 2017.

[4] Y. Levy. Intrinsically disordered regions as affinity tuners in protein-DNA interactions. *Biophysical journal*, 102(3):632a–632a, 2012.

[5] D.R.G. Subekti, A. Murata, Y. Itoh, S. Fukuchi, H. Takahashi, S. Kanbayashi, S. Takahashi, and K. Kamagata. The disordered linker in p53 participates in nonspecific binding to and one-dimensional sliding along DNA revealed by single-molecule fluorescence measurements. *Biochemistry (Easton)*, 56(32):4134–4144, 2017.

[6] V.N. Uversky, C.J. Oldfield, and A.K. Dunker. Intrinsically disordered proteins in human diseases: Introducing the D2 concept. 37(1):215–246, 2008.

[7] A.C. Joerger and A.R. Fersht. The tumor suppressor p53: From structures to drug discovery. *Cold Spring Harbor perspectives in biology*, 2(6):a000919–a000919, 2010.

[8] V. N. Uversky. Natively unfolded proteins: A point where biology waits for physics. *Protein science*, 11(4):739–756, 2002.

[9] P.E. Wright and H.J. Dyson. Intrinsically disordered proteins in cellular signalling and regulation. *Nature reviews. Molecular cell biology*, 16(1):18–29, 2014.

[10] H.J. Dyson and Wright P.E. Intrinsically unstructured proteins and their functions. *Nature Reviews Molecular Cell Biology*, 6(3):197, 2005.

[11] R. van der Lee, M. Buljan, B. Lang, R.J. Weatheritt, G.W. Daughdrill, A.K. Dunker, M. Fuxreiter, J. Gough, J. Gsponer, D.T. Jones, P.M. Kim, R.W. Kriwacki, C.J. Oldfield, R.V. Pappu, P. Tompa, V.N. Uversky, P.E. Wright, and M.M. Babu. Classification of intrinsically disordered regions and proteins. *Chemical Reviews*, 114(13):6589–6631, 2014.

[12] J.C. Wootton. Sequences with “unusual" amino-acid compositions. *Current Opinion In Structural Biology*, 4(3):413–421, 1994.

[13] P. Romero, Z. Obradovic, X. Li, E.C. Garner, C.J. Brown, and A.K. Dunker. Sequence complexity of disordered protein. *Proteins: Structure, Function, and Bioinformatics*, 42(1):38–48, 2001.

[14] V.N. Uversky. The intrinsic disorder alphabet. iii. dual personality of serine. *Intrinsically Disordered Proteins*, 3(1):e1027032–e1027032, 2015.

[15] P. Tompa. Intrinsically unstructured proteins. *Trends in Biochemical Sciences*, 27(10):527–533, 2002.

[16] M.-L. Ainalem and T. Nylander. DNA condensation using cationic dendrimers—morphology and supramolecular structure of formed aggregates. *Soft Matter*, 7:4577–4594, 2011.

[17] International Human Genome Sequencing Consortium. Finishing the euchromatic sequence of the human genome. *Nature*, 431(7011):931, 2004.

[18] C.W. Garvie and C. Wolberger. Recognition of specific DNA sequences. *Molecular Cell*, 8(5):937–946, 2001.

[19] N.M. Luscombe, R.A. Laskowski, and J.M. Thornton. Amino acid-base interactions: a three-dimensional analysis of protein-DNA interactions at an atomic level. *Nucleic Acids Research*, 29(13):2860–2874, 2001.

[20] J. Ha, R.S. Spolar, and M.T. Record. Role of the hydrophobic effect in stability of site-specific protein-DNA complexes. *Journal of molecular biology*, 209(4):801–816, 1989.

[21] D. Normanno, L. Boudarène, C. Dugast-Darzacq, J. Chen, C. Richter, F. Proux, O. Bénichou, R. Voituriez, X. Darzacq, and M. Dahan. Probing the target search of DNA-binding proteins in mammalian cells using tetr as model searcher. *Nature communications*, 6(1):7357–7357, 2015.

[22] A. Ganguly, P. Rajdev, S.M. Williams, and D. Chatterji. Nonspecific interaction between DNA and protein allows for cooperativity: A case study with mycobacterium DNA binding protein. *The journal of physical chemistry. B*, 116(1):621–632, 2012.

[23] C.G. Kalodimos. Structure and flexibility adaptation in nonspecific and specific protein-DNA complexes. *Science (American Association for the Advancement of Science)*, 305(5682):386–389, 2004.

[24] S.E. Halford and J.F. Marko. How do site-specific DNA-binding proteins find their targets? *Nucleic acids research*, 32(10):3040–3052, 2004.

[25] M. Doucleff and G.M. Clore. Global jumping and domain-specific intersegment transfer between DNA cognate sites of the multidomain transcription factor Oct-1. *Proceedings of the National Academy of Sciences*, 105(37):13871, 2008.

[26] Y. Gao, Y.H. Foo, R.S. Winardhi, Q. Tang, J. Yan, and L.J. Kenney. Charged residues in the H-NS linker drive DNA binding and gene silencing in single cells. *Proceedings of the National Academy of Sciences*, 2017.

[27] C.J. Brown, S. Lain, C.S. Verma, A.R. Fersht, and D.P. Lane. Awakening guardian angels: drugging the p53 pathway. *Nature reviews. Cancer*, 9(12):862–873, 2009.

[28] K. Kamagata, A. Murata, Y. Itoh, and S. Takahashi. Characterization of facilitated diffusion of tumor suppressor p53 along DNA using single-molecule fluorescence imaging. *Journal of photochemistry and photobiology. C, Photochemistry reviews*, 30:36–50, 2017.

[29] A. Tafvizi, F. Huang, A.R. Fersht, L.A. Mirny, and A.M. van Oijen. A single-molecule characterization of p53 search on DNA. *Proceedings of the National Academy of Sciences - PNAS*, 108(2):563–568, 2011.

[30] K. McKinney, M. Mattia, V. Gottifredi, and C. Prives. p53 linear diffusion along DNA requires its C terminus. *Molecular cell*, 16(3):413–424, 2004.

[31] R.V. de Araújo, S. da Silva Santos, E. Igne Ferreira, and J. Giarolla. New advances in general biomedical applications of PAMAM dendrimers. *Molecules*, 23(11), 2018.

[32] Z. Lyu, L. Ding, A.Y.-T. Huang, C.-L. Kao, and L. Peng. Poly(amidoamine) dendrimers: covalent and supramolecular synthesis. *Materials Today Chemistry*, 13:34 – 48, 2019.

[33] D. Cakara, J. Kleimann, and M. Borkovec. Microscopic protonation equilibria of poly(amidoamine) dendrimers from macroscopic titrations. *Macromolecules*, 36(11):4201–4207, 2003.

[34] U. Böhme, A. Klenge, B. Hänel, and U. Scheler. Counterion condensation and effective charge of PAMAM dendrimers. *Polymers*, 3(2):812–819, 2011.

[35] M.-L. Örberg, K. Schillén, and T. Nylander. Dynamic light scattering and fluorescence study of the interaction between double-stranded DNA and poly(amido amine) dendrimers. *Biomacromolecules*, 8(5):1557–1563, May 2007.

[36] K. Fant, E.K. Esbjörner, P. Lincoln, and B. Nordén. DNA condensation by PAMAM dendrimers: Self-assembly characteristics and effect on transcription. *Biochemistry*, 47(6):1732–1740, 2008.

[37] K. Wagner, D. Harries, S. May, V. Kahl, J.O. Rädler, and A. Ben-Shaul. Direct evidence for counterion release upon cationic lipid DNA condensation. *Langmuir*, 16(2):303–306, 2000.

[38] S.M. Mel'nikov, M.O. Khan, B. Lindman, and B. Jönsson. Phase behavior of single dna in mixed solvents. *Journal of the American Chemical Society*, 121(6):1130–1136, 1999.

[39] M.-L. Ainalem, A.M. Carnerup, J. Janiak, V. Alfredsson, T. Nylander, and K. Schillén. Condensing DNA with poly(amido amine) dendrimers of different generations: means of controlling aggregate morphology. *Soft Matter*, 5:2310–2320, 2009.

[40] J.R. Lakowicz. *Principles of Fluorescence Spectroscopy*. Springer, Boston, 2006.

[41] J.W. Lichtman and J.-A. Conchello. Fluorescence microscopy. *Nature methods*, 2(12):910–919, 2005.

[42] L.O. Narhi, I. Rayment, and N. Allewell. *Molecular Biophysics for the Life Sciences*, volume 6 of *Biophysics for the Life Sciences*. Springer New York, New York, NY, 2013 edition, 2013.

[43] J.M. Parnis and K.B. Oldham. Beyond the Beer–Lambert law: The dependence of absorbance on time in photochemistry. *Journal of photochemistry and photobiology. A, Chemistry.*, 267:6–10, 2013.

[44] D. Sheehan. *Physical biochemistry : principles and applications*. Wiley Blackwell, Chichester, 2nd ed. edition, 2009.

[45] K.E. Van Holde. *Principles of physical biochemistry*. Pearson/Prentice Hall, Upper Saddle River, N.J, 2nd ed. edition, 2006.

[46] S. Sun, W. Liu, N. Cheng, B. Zhang, Z. Cao, K. Yao, D. Liang, A. Zuo, G. Guo, and J. Zhang. A thermoresponsive chitosannipaam/vinyl laurate copolymer vector for gene transfection. *Bioconjugate chemistry*, 16(4):972–980, 2005.

[47] M. Mann, R.C. Hendrickson, and A. Pandey. Analysis of proteins and proteomes by mass spectrometry. *Annual review of biochemistry*, 70(1):437–473, 2001.

[48] J.H. Gross. *Mass spectrometry : a textbook*. Springer, Cham, Switzerland, 3rd edition, 2017.

[49] S. Banerjee and S. Mazumdar. Electrospray ionization mass spectrometry: A technique to access the information beyond the molecular weight of the analyte. *International journal of analytical chemistry*, 2012:282574–40, 2012.

[50] A. Uclés, M.M. Ulaszewska, M.D. Hernando, M.J. Ramos, S. Herrera, E. García, and A.R. Fernández-Alba. Qualitative and quantitative analysis of poly(amidoamine) dendrimers in an aqueous matrix by liquid chromatography–electrospray ionization-hybrid quadrupole/time-of-flight mass spectrometry (LC-ESI-QTOF-MS). *Analytical and bioanalytical chemistry*, 405(18):5901–5914, 2013.

[51] S. McIndoe and K.L. Vikse. Assigning the ESI mass spectra of organometallic and coordination compounds. *Journal of mass spectrometry.*, 54(5):ii–ii, 2019.

[52] J.L. Santos, D. Pandita, J. Rodrigues, A.P. Pêgo, P.L. Granja, G. Balian, and H. Tomás. Receptor-mediated gene delivery using PAMAM dendrimers conjugated with peptides recognized by mesenchymal stem cells. *Molecular pharmaceutics*, 7(3):763–774, 2010.

[53] C.L. Waite and C.M. Roth. PAMAM-RGD conjugates enhance siRNA delivery through a multicellular spheroid model of malignant glioma. *Bioconjugate Chemistry*, 20(10):1908–1916, 2009.

[54] Thermo Fisher Scientific, Pierce Biotechnology *SPDP Crosslinkers*, 2011. https://www.thermofisher.com/document-connect/document-connect.html?url=https%3A%2F%2Fassets.thermofisher.com%2FTFS-Assets%2FLSG%2Fmanuals%2FMAN0011212_SPDP_CrsLnk_UG.pdf&title=VXNlciBHdWlkZTogIFNQRFAgQ3Jvc3NsaW5rZXJz. Accessed: 26.01.21.

[55] Thermo Fisher Scientific, Pierce Biotechnology. *PageBlue Protein Staining Solution*, 2017. https://www.thermofisher.com/document-connect/document-connect.html?url=https%3A%2F%2Fassets.thermofisher.com%2FTFS-Assets%2FLSG%2Fmanuals%2FMAN0011813_PageBlue_Protein_Stain_Solution_UG.pdf&title=VXNlciBHdWlkZTogIFBhZ2VCbHVlIFByb3RaW4gU3RhaW5pbmcgU29sdXRpb24=. Accessed: 28.01.21.

[56] Y. Cheng, Q. Wu, Y. Li, J. Hu, and T. Xu. New insights into the interactions between dendrimers and surfactants: 2. design of new drug formulations based on dendrimersurfactant aggregates. *The journal of physical chemistry. B*, 113(24):8339–8346, 2009.

[57] A. Sharma, A. Desai, R. Ali, and D. Tomalia. Polyacrylamide gel electrophoresis separation and detection of polyamidoamine dendrimers possessing various cores and terminal groups. *Journal of Chromatography A*, 1081(2):238–244, 2005.

[58] M.-L. Ainalem, A. Bartles, J. Muck, R.S. Dias, A.M. Carnerup, D. Zink, and T. Nylander. DNA compaction induced by a cationic polymer or surfactant impact gene expression and DNA degradation. *PloS one*, 9(3):e92692–e92692, 2014.

[59] N. Tahallah, M. Pinkse, C.S. Maier, A.J.R. Heck, and J.A. Loo. The effect of the source pressure on the abundance of ions of noncovalent protein assemblies in an electrospray ionization orthogonal time-of-flight instrument. *Rapid communications in mass spectrometry*, 15(8):596–601, 2001.

[60] N.V. Bhagavan. *Essentials of medical biochemistry : with clinical cases*. Elsevier Academic Press, 2015.

Appendix

A.1 Mass spectrometry - Full retention time

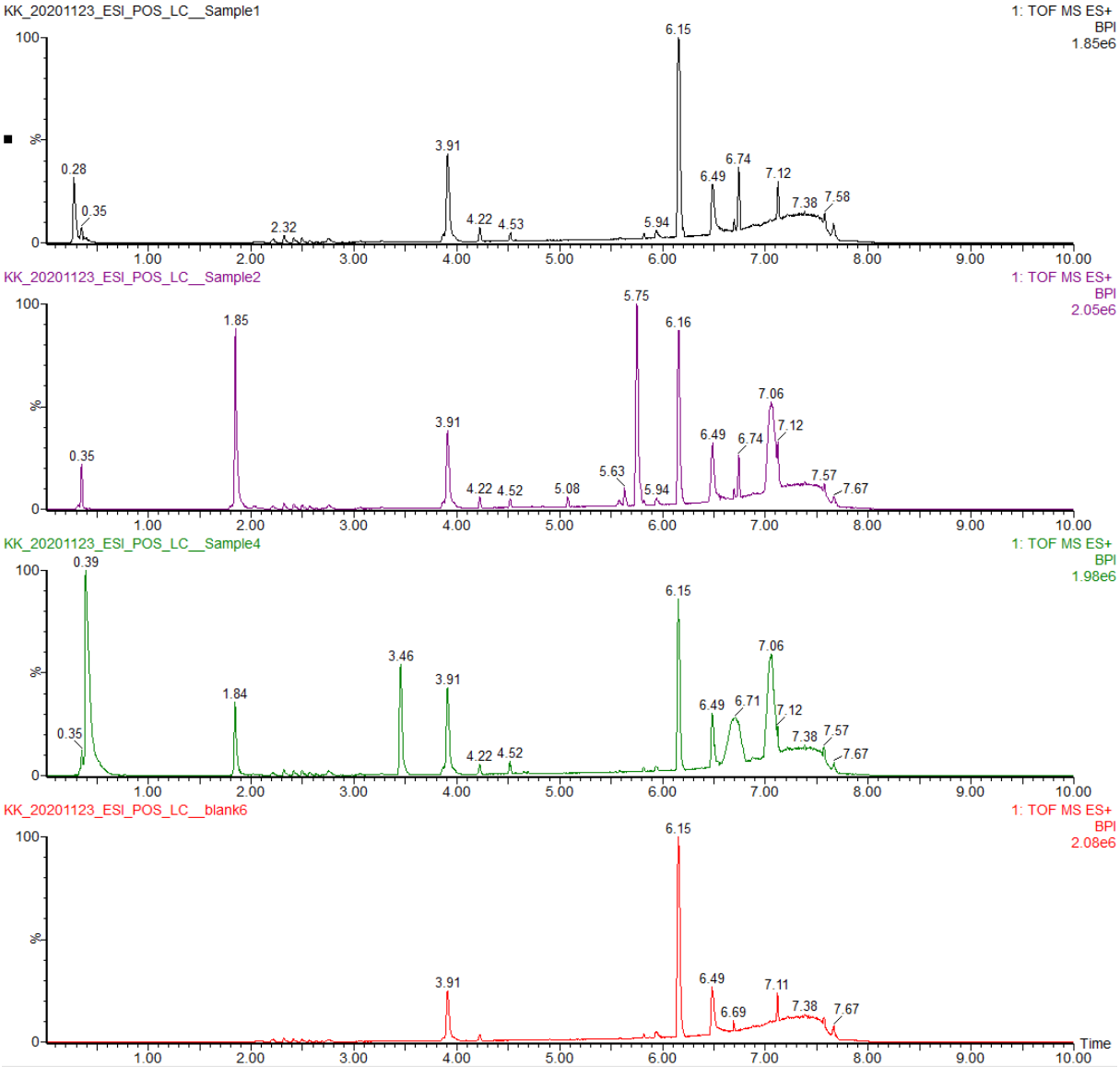

Figure A.1: Intensity as a function of retention time for the chromatographic separation of solutions in mass spectrometry. From top to bottom panel, the graphs correspond to PAMAM, SN8-24 peptide, PAMAM-SN8-24 conjugate and blank.

A.2 Additional dye exclusion assay of PAMAM-SN8-24 and DNA

Figure A.2 shows the dye exclusion assay performed for PAMAM-SN8-24 conjugates and salmon sperm DNA. Control samples were made with SN8-24 and DNA with GelStar, and PAMAM-SN8-24 with GelStar (not shown). The intensity of the sample containing SN8-24 and DNA was approximately 1, thus the peptide did not condense the DNA or bind GelStar. The intensity for PAMAM-SN8-24 and GelStar was close to 0, indicating that the conjugate did not bind GelStar.

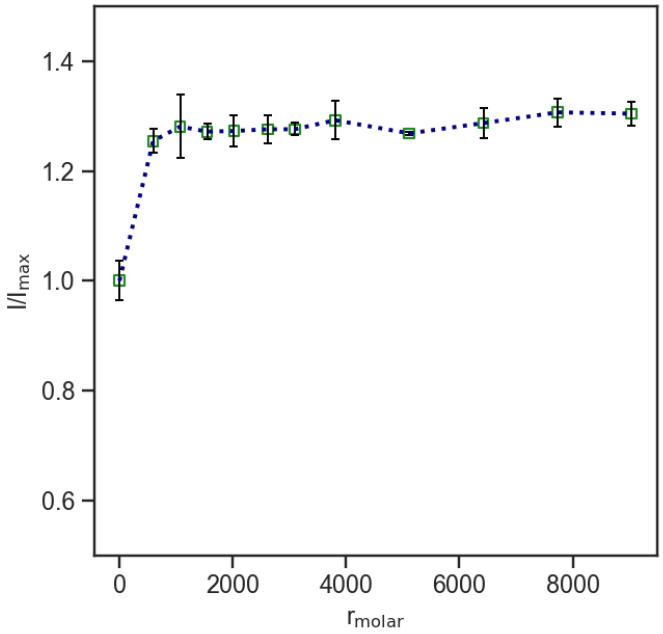

Figure A.2: Normalized fluorescence intensity as a function of r_{molar}. The assay was performed for increasing concentration of PAMAM-SN8-24 conjugates and constant DNA concentration.

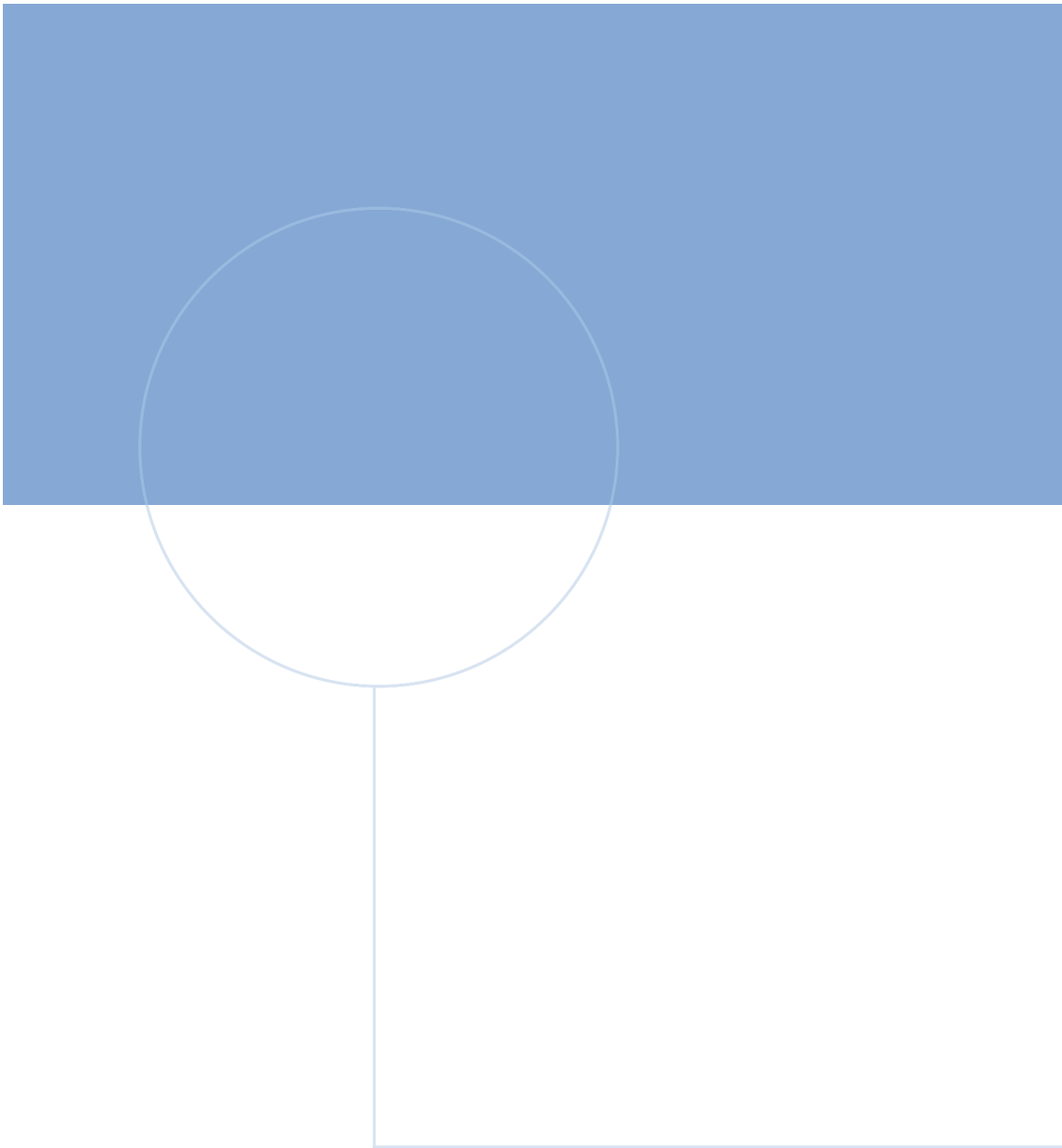

NTNU

Norwegian University of
Science and Technology